CHAPTER 1

Introduction

For millennia mankind has watched and studied the night sky. Apart from planets and comets it appeared as an immutable canvas on which the stars rested. It comes as no surprise that for ancient civilisations supernovae (which were very rare events, occurring only every few centuries) were interpreted as important omens as they broke the paradigm of the unchanging night skies. As these events are so rare their origin remained a mystery until in the first half of the last century. Baade & Zwicky (1934) suggested that *"the phenomenon of a super-nova represents the transition of an ordinary star into a body of considerably smaller mass"*. For the last 85 years the supernova-branch of astronomy has been developing. There have been many advances, but there are still many unknowns. This thesis addresses two sub fields of supernovae: The unsolved progenitor problem for Type Ia supernovae as well as quantifying the nucleosynthetic yield and energies of Type Ia supernovae.

1.1. Ancient Supernovae

Although supernovae must have been observed since the beginning of humankind, reliable records only exist for the last thousand years. There are however transient star sightings mentioned in older text. For example, *Houhanshu* (Zhao et al., 2006), mentions a new star which was visible for 8 months (depending on the interpretation of the text it could also mean 20 months) in the year of AD185. This new star was reported to be in the *Nanmen* asterism which is close to Alpha Centauri. Observations in modern times have revealed a supernova remnant in a distance of roughly 1 kpc near Alpha Centauri (Zhao et al., 2006). Some believe this to be evidence that the star mentioned in the ancient text is the oldest written record of a supernova, others however interpret this text as reference to a comet (Chin & Huang, 1994).

The oldest undisputed record of a supernova is SN 1006, which also coincides with the brightest ever recorded supernova. It was observed worldwide by Asian, Arabic and European astronomers. Goldstein (1965) gives a good summary of the observations and interpretation given by these ancient observers. Ali Ibn Ridwan was an Egyptian astronomer who recorded the appearance of SN 1006. He wrote in a comment on Ptolemy's Tetrabiblos:

> *"I will now describe for you a spectacle that I saw at the beginning of my education. This spectacle appeared in the zodiacal sign Scorpio in opposition to the sun, at which*

Figure 1.1 Chaco canyon petroglyphs show a hand, a moon and a bright celestial object. This could be SN1054 but it is ambiguous. (Source Wikipedia/ Photographer jamesdale10/ Creative Commons license)

> *time the sun was in the 15th degree of Taurus, and the spectacle in the 15th degree of Scorpio. It was a large spectacle, round in shape and its size 2.5 or 3 times the magnitude of Venus. Its light illuminated the horizon and twinkled very much. ... This apparition was also observed at the time by (other) scholars just as I have recorded it."*

Only 50 years after the bright supernova of 1006, Chinese and Japanese astronomers reported on another cataclysmic event which was at first even visible during the day. SN 1054 might have also been observed in North America where petroglyphs in the Chaco Canyon could be interpreted as a depiction of this event (see Figure 1.1). It is difficult to date these cave paintings precisely, but they were created around the time of the SN 1054 explosion. It is still debated if SN 1054 was the inspiration of the painting or the inspiration came from the passing of Hailey's comet in 1066. More than 900 years later Staelin & Reifenstein (1968) detected a pulsar in the centre of SN 1054. This was the first time that the stellar remnant connected with a known supernova was found. SN 1181 ends the 180 year period with three confirmed supernovae that started with SN 1006. This Galactic supernovae first discovered in August of 1181 was visible for about half a year and was mentioned in eight different texts by Chinese and Japanese astronomers. 3C58, a pulsar found in SN 1181, is suggested to be the neutron star remnant of this stellar explosion.

Humanity had to wait for nearly 400 years before the next bright event occurred. Although the supernova was discovered by an abbot in Messina on 06 November 1572, Tycho Brahe is often attributed the discovery of this event. The attribution of SN 1572 to Tycho came from his angular distance and brightness measurements of unprecedented

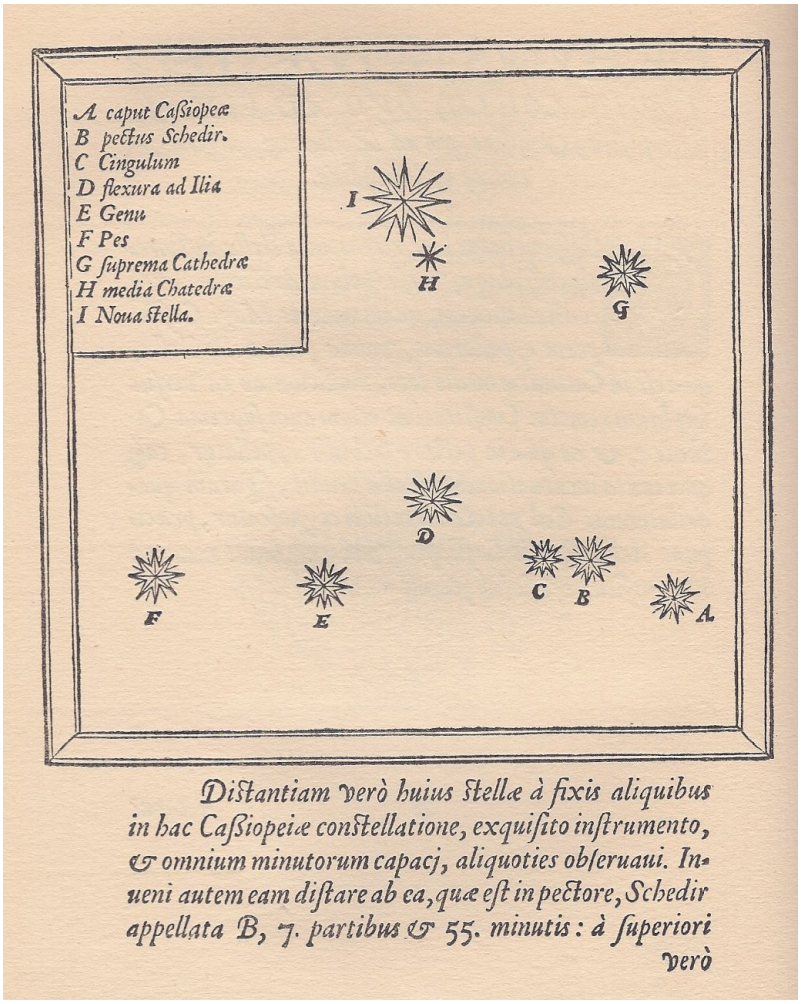

Figure 1.2 Brahe, Tychonis [A facsimile reprint of the original edition, 1573]. The supernova is marked with the letter I. The caption reads: *"I have indeed measured the distance of this star from some of the fixed stars in the constellation of Cassiopeia several times with an exquisite (optical) instrument, which is capable of all the fine details of measurement. I have further detected that it (the new star) is located 7 degrees and 55 minutes from the star at the breast of the Schedir designated by B."* translation kindly provided by Leonhard Kretzenbacher

precision (location to a few arc minutes!; see Figure 1.2). These precise measurements proved that the star changed in brightness but stayed at a fixed position like stars. Therefore Tycho concluded that this transient event was far beyond the moon, where stars were suspected to be located. This broke the paradigm of the constancy of stars, which was believed by many. Having been studied for almost one and a half years the supernova finally faded from visibility in March 1574. The measurements of SN 1572, among other astronomy related subjects, were published by Brahe & Kepler (1602). Another 400 years elapsed before radio emissions identified the remains of SN 1572 (Hanbury Brown & Hazard, 1952).

Kepler, working with Tycho, discovered SN 1604 nearly 20 days before maximum light, which occurred on the 28th of October 1604. Serendipitously, around this time there was a conjunction of Jupiter and Mars, which was observed by many astronomers. This also led to an early upper limit, where astronomers described the conjunction but did not mention

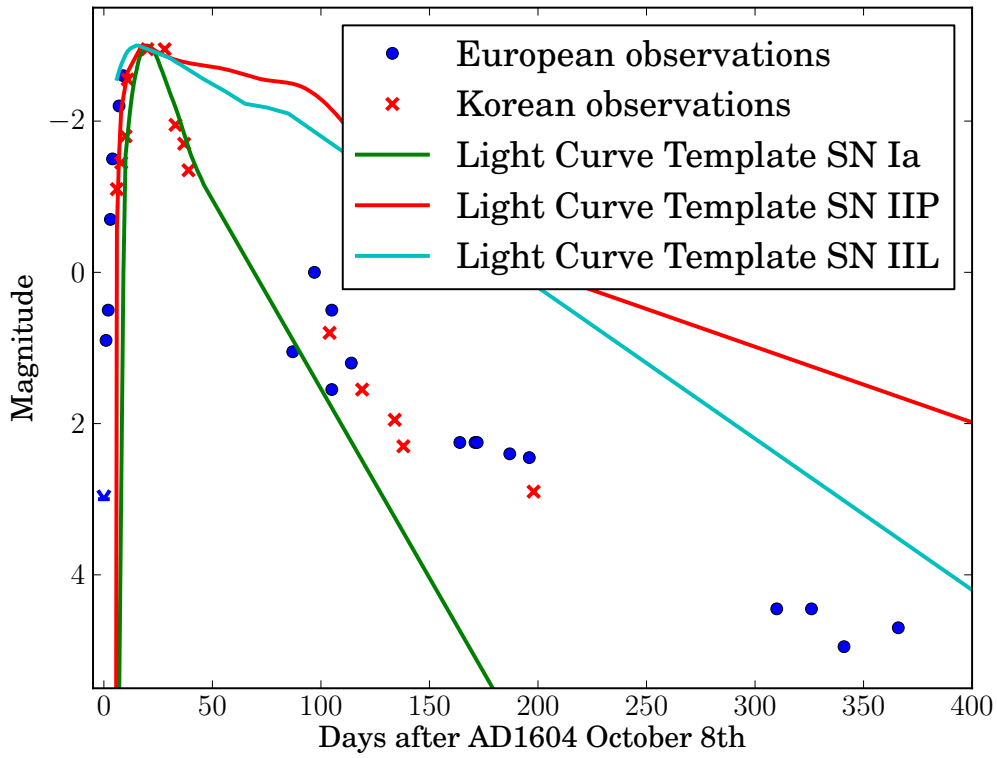

Figure 1.3 Light curve of SN 1604 obtained by ancient European and Korean astronomers. There is a European upper limit on the 8th of October 1604. Comparing these 400 year old measurements with modern day light curve templates by Li et al. (2011) show clearly that the supernova is a Type Ia supernova. Historical data graciously supplied by D.A. Green (Clark & Stephenson, 1977; Green & Stephenson, 2003)

the supernova. As Tycho did before him, Kepler measured the location and the brightness of the supernova precisely (see Figure 1.3; Kepler, 1606) before it faded from visibility 18 months later. Kepler was not the only astronomer observing SN 1604 and there exist many texts from Korea and China mentioning this event. SN 1604 was the last confirmed observation of a supernova in our own Galaxy. A good review of these ancient supernovae can be found in Green & Stephenson (2003).

Observations in modern times have revealed two additional supernovae that must have exploded after SN 1604 but are not mentioned in the historical literature. Cas A, a supernova remnant, is the brightest radio source in the sky. It has been estimated that this supernova should have been visible between 1660 and 1680, however there are no clear descriptions or references from astronomers in the seventeenth century. There has been much speculation to the reason (e.g. heavily obscured by interstellar dust and thus not visible), but it still remains unclear why it was not observed. Green & Gull (1984) detected another supernova remnant right in the heart of our Galaxy. Recent X-ray observations revealed the supernova to be less than 150 years old (Reynolds et al., 2008). This supernova happened very close to the galactic centre and is heavily obscured by dust. At the time of explosion it was not visible at optical wavelengths. In summary, the five ancient supernovae (SN 1006, SN 1054, SN 1181, SN 1572 and SN 1604) were all

observed without the use of a telescope. Our ancient astronomy colleagues had only very primitive means to observe supernovae. However, the remarkably precise written records can be attributed to their ingenuity and assiduity. Even in an era of 10-meter telescopes the records of these explosions remain useful (see Figure 1.3).

1.2. Modern Supernova Observations and Surveys

The era of modern supernova observations started with the discovery of SN 1885. SN 1885 (also known as S Andromedae) was first spotted by Isaac Ward in Belfast in August of 1885 (Hartwig, 1885) and was visible until February 1886. More than 50 years later Baade & Zwicky (1934) coined the term supernova and established the difference between common novae and supernovae. Baade & Zwicky (1934) also suggested that these luminous events are caused by the deaths of stars.

In order to understand the phenomenon of supernovae better, Zwicky began a supernova search with the 18-inch Schmidt telescope. In those days the detectors were photographic plates, which were analysed with the help of a blink comparator. This device permitted rapid switching between viewing two different photographic plates which were observed on different nights and one could easily detect *new stars*. Using this method Zwicky found several supernovae which in turn inspired Minkowski to classify these supernovae by their spectra (Minkowski, 1941). Minkowski categorised the 14 known objects into two categories. Those without hydrogen he called *Type I*, those with hydrogen he called *Type II* (see Section 1.3.1 for a more detailed description of supernova classification).

With the advent of computing in the 1960s the first computer-controlled telescopes were built. A 24-inch telescope was constructed by the Northwestern University and deployed at the Corralitos Observatory in New Mexico with the express purpose of undertaking a Digitized Astronomy Supernova Survey (DASS; Colgate et al., 1975). While ultimately unsuccessful in finding supernovae, this search lead the way in computer controlled discovery and many later surveys would employ a similar design.

The advancements of detector technologies in 1980s, such as photoelectric photometers and later charged coupled devices (CCDs), together with increasing power and connectivity of computers, enabled the construction of automated telescopes with minimal human interaction (e.g. Genet et al., 1986). These first automated telescopes were used mainly for variable star surveys.

The Berkley Automatic Imaging Telescope (BAIT; Richmond et al., 1993) was one of the first automated telescopes designed specifically to find supernovae. This search produced 15 supernova discoveries by 1994 (van Dyk et al., 1994), including the famous SN 1994D, pictured here (Figure 1.4). Due to increasing light pollution in Berkley this project moved to the Lick Observatories and was named the Lick Observatory Supernova Search (LOSS; Li et al., 2000). With the switch to the new observatory the BAIT was replaced with the Katzman Automatic Imaging Telescope (KAIT; Filippenko et al., 2001). LOSS has been one of the most successful supernova surveys to date. By the year 2000 it had found 96 supernovae (Filippenko et al., 2001).

In the mid to late 1990s, as high quality data on supernovae became available (mainly contributed by the Calán/Tololo supernova survey (CTSS; Hamuy et al., 1993)), the long dream (e.g. Baade, 1938; van den Bergh, 1960; Kowal, 1968) of using these objects as reliable distance indicators finally became viable. Two main teams drove the advancement in the

Figure 1.4 SN 1994D in NGC 4526 taken with the same HST. This image shows very clearly how the light from the explosion of only one star can outshine an entire galaxy (Pete Challis/NASA). This picture is also widely used in popular astronomy.

cosmological distance measurements (the Supernova Cosmology Project (SCP) and the High Z Supernova Search (HZSNS)) and independently arrived at the same conclusion: the expansion of the universe is accelerating (Riess et al., 1998; Perlmutter et al., 1999). For a more detailed overview of supernova cosmology see Section 1.3.6.

By the turn of the millennium and following the discovery of the accelerated expansion of the universe, a variety of groups started large surveys specifically for supernovae. Among them were the 'The Equation of State: SupErNovae trace Cosmic Expansion' (ESSENCE; Garnavich et al., 2002) project and Supernova Legacy Survey (SNLS; Pain & SNLS Collaboration, 2003). Both these programs have finished taking data, but have yet to publish all of their observations. Specialised surveys like the Nearby Supernova Factory (Aldering et al., 2002) used an Integral Field Unit (IFU) to capture light curves and spectra at the same time. The Higher-z survey (Strolger et al., 2004) focused on a high redshift

range, available only through the HST.

This effort is continued by a multitude of large sky surveys that have started in recent years (or are just about to). Some of these focus exclusively on transients and supernovae, like the Palomar Transient Factory (PTF; Rau et al., 2009), whereas others, like the Panoramic Survey Telescope & Rapid Response System (PanSTARRS; Kaiser, 2004) and SkyMapper (Keller et al., 2007), have transient/supernova components. Upcoming surveys, like the Large Synoptic Survey Telescope (LSST; Pinto et al., 2006) and the space-based Global Astrometric Interferometer for Astrophysics (GAIA; Perryman et al., 2001) mission, will provide unprecedented detail about current supernova types as well finding several new classes of transients (e.g. GAIA will find $\approx 14,000$ Type Ia supernovae (SNe Ia) during its mission lifetime; Belokurov & Evans, 2003).

In addition to supernova searches in the optical, searches have commenced at other wavelengths and other physical messengers. Gamma Ray Bursts (GRBs) were first detected, as the name suggests, in gamma-rays and are thought to be the bolometrically brightest transients. The first detection of a GRB was on July 2 of 1967 by a Vela satellite. Vela satellites where designed to monitor gamma-ray signatures of banned nuclear weapons testing. It became quickly clear, due to the unusual form and direction of the signal, that these new GRBs where not of terrestrial origin. Six years later, the results from the Vela satellites were declassified and the existence of these GRBs made known to the world (Klebesadel et al., 1973).

At the beginning of the 1990s, new high-energy instruments like the Burst and Transient Source Experiment (BATSE) surveyed the sky in gamma-rays and detected thousands of GRBs. Meegan et al. (1992) showed that GRBs, due to their isotropic distribution, are events at cosmological distances rather than coming from our own Galaxy. The BeppoSAX satellite, launched in 1996, was able to provide accurate positions for GRBs. This advancement led to the discovery that GRBs occur in distant galaxies, establishing them as one of the most luminous events in the universe ($> 10^{52}$ erg). The co-location of SN 1998bw and GRB 980425 established the connection between supernovae and some GRBs (Galama et al., 1998). A class of short GRBs has remained supernovaless (Xu et al., 2009, e.g.). The subsequent High Energy Transient Explorer (HETE) mission established a new class of transients called X-ray-flashes. These new objects are thought to be similar to GRBs in physical nature but much less energetic (Zhang et al., 2004). Such work continues with the Swift mission.

Astronomy has been largely based on electromagnetic waves, but there are other messengers of astrophysical information. Gravitational waves, predicted by the theory of general relativity (Einstein, 1918), might provide us with another insight into supernovae. The most advanced detector today, the Laser Interferometer Gravitational Wave Observatory (LIGO; Abramovici et al., 1992) has not yet detected gravitational waves, although modelling indicates that it would have been highly unlikely, to have an event close enough to have been detected by LIGO. Advanced LIGO will likely detect gravitational waves from in-spiralling neutron stars, and possibly core collapse supernovae. The Laser Interferometer Space Antenna (LISA; Jafry et al., 1994), an ambitious mission planned for the coming decade, is definitely sensitive enough to detect the predicted gravitational waves (a non-detection would show problems with the theory of general relativity). In the supernova field LISA might give us an estimate on the number of in-spiralling white dwarfs, which are suggested as progenitors of SNe Ia.

SN 1987A was the first and only occasion on which neutrino emission from a supernova has been measured (Bionta et al., 1987; Hirata et al., 1987; Alekseev et al., 1988). New, more sensitive detectors, like IceCube (Karle, 2008), will hopefully enable accurate neutrino observations of future Galactic supernovae.

For now, the optical observations of supernovae provide the bulk of observations of these transients. Hopefully, future instruments and capabilities will enable us to combine measurements across the electromagnetic spectrum with gravitational wave and particle flux observations. Such an approach will unlock many of the secrets still held by these mysterious objects.

1.3. Observational Properties of Supernovae

1.3.1. Supernova classification

The classification of supernovae started in 1941 when Minkowski realised that there seem to be two main types (Minkowski, 1941). Those containing a Hα line he called Type II supernovae and those showing no hydrogen he called Type I supernovae. This basic classification has remained to this day, however the two main classes branched into several subclasses. During the 1980s, the community discovered that most SNe Ia showed a broad Si II line at 6130 Å. There was, however, a distinct subclass of objects that lacked this feature. These silicon-less objects were then subclassed further into objects that showed helium – now known as Type Ib supernova (SN Ib) – and those that did not, called Type Ic supernova (SN Ic) (see spectra in Figure 1.5; Harkness et al., 1987; Gaskell et al., 1986). The classical Type I supernova was renamed to SN Ia. Today we know that SNe Ia originate from the explosion of white dwarfs. Type II supernovae (SNe II) and Type Ib/c supernovae (SNe Ib/c) are believed to stem from the collapsing core of a massive star.

Only in the past two decades have we been able to explore the finer details of the SNe Ia class. Most objects have a small brightness scatter and are referred to as *Branch-normal* SNe Ia (Branch et al., 1993). In this class of *Branch-normal* SNe Ia, the community has found additional features that vary with brightness. For example, Benetti et al. (2005) found that the evolution of the photospheric velocity measured from the Doppler shift of the Si II line at 6355 Å is faster in more luminous SNe Ia (high velocity gradient - HVG) and slower in fainter SNe Ia (low velocity gradient - LVG) . Additionally, the luminosity of SNe Ia manifests itself in the spectra through the ratio of the Si II absorption features at 5800 Å and the feature at 6150Å (Nugent et al., 1995). Whereas faint supernovae have a pronounced trough at 5800 Å the luminous ones completely lack this feature but show a strong absorption line at 6150 Å instead.

In addition to the group of *Branch-normal* SNe Ia, there are more distinct subclasses with extreme luminosities and peculiar spectra. The overluminous class we call 91T-like after the bright supernova SN 1991T (Phillips et al., 1992). In their spectra, 91T-like SNe Ia at early times show weak silicon and calcium lines, leading to a nearly featureless continuum. At late times this class shows a spectrum similar to *Branch-normal* SNe Ia. The faint supernova SN 1991bg (Filippenko et al., 1992) is the namesake for the underluminous class (91bg-like). 91bg-like SNe Ia are characterised spectroscopically by their distinct lack of strong iron group element (IGE) features. A third prominent subclass (see Figure 1.7) is the 02cx-like SNe Ia (Li et al., 2003) SNe Ia named after SN 2002cx. Observationally, they can be seen

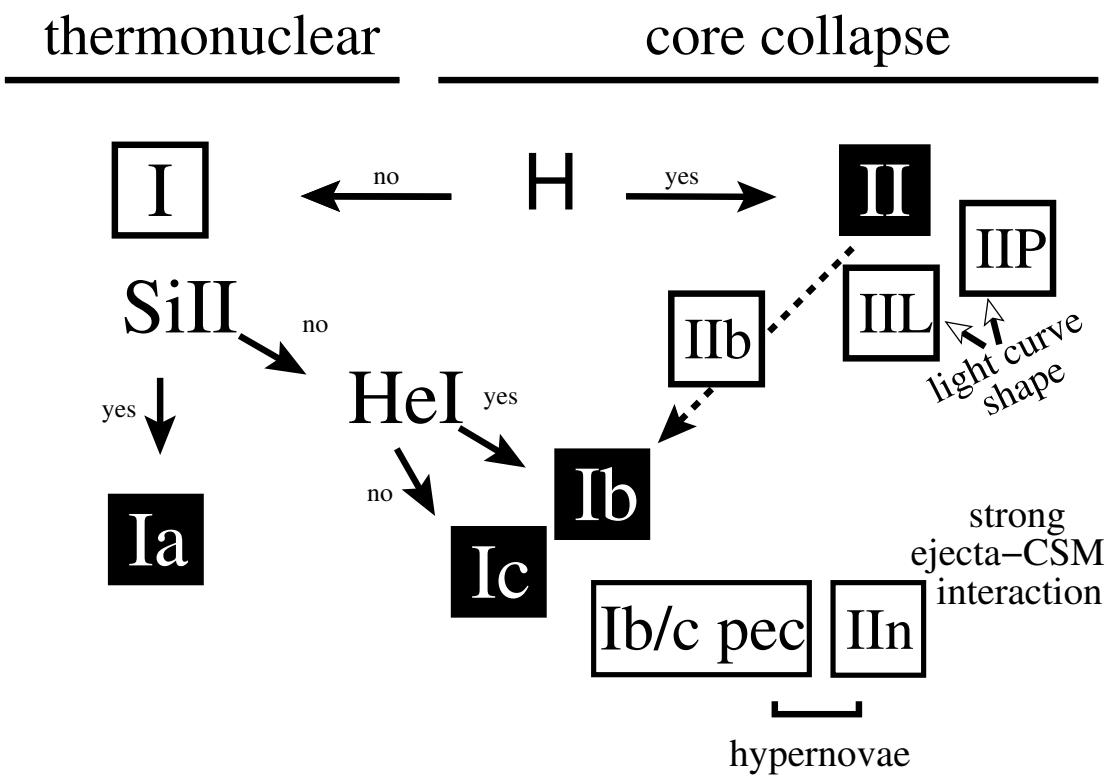

Figure 1.5 Classification scheme by Turatto (2003)

as a chimera between 91bg-like SNe Ia and 91T-like SNe Ia, inheriting the low luminosity from the former and the pre-maximum featureless continuum from the latter. In addition, 02cx-like spectra are dominated by IGE features. Li et al. (2011) have measured the fraction of different subclasses from the LOSS dataset. Figure 1.7 shows the fraction of the different subclasses that would be expected from a purely magnitude limited search. Although there are several different subclasses, the class of SNe Ia is relatively homogeneous as it is dominated by the *Branch-normal* SNe Ia- in stark contrast to the different SNe II.

SNe II span large ranges in observables. We can divide the main class into four subclasses. Type II Plateau supernovae (SNe IIP; Barbon et al., 1979) have a relatively flat light curve after an initial maximum (see Figure 1.9). In contrast the Type II Linear supernovae (SNe IIL; Schlegel, 1990) have a rapid linear decline after the maximum. The third subclass is the Type II narrow-lined supernova (SN IIn) which is characterised by narrow emission lines, which are thought to come from interaction with the circumstellar medium (CSM). Finally the Type IIb supernovae (SNe IIb) show strong hydrogen lines in their early spectrum, but evolve to become spectroscopically more like SNe Ib with no hydrogen lines but strong silicon and helium lines. SNe Ib and SNe Ic (often referred to as SNe Ib/c) are believed to originate from the same physical process as all SN II-classes - the collapse of stellar cores (often grouped as SN II/Ib/c). In contrast to the SNe Ia, which are dominated by one subclass (*Branch-normal* SNe Ia), the different subclasses of SNe II are much more uniformly distributed (see Figure 1.8). But the classes are also much less strict with numerous intermediate and some peculiar objects. For a more comprehensive review of the classification of supernovae the reader should consult Turatto (2003) and Turatto et al. (2007).

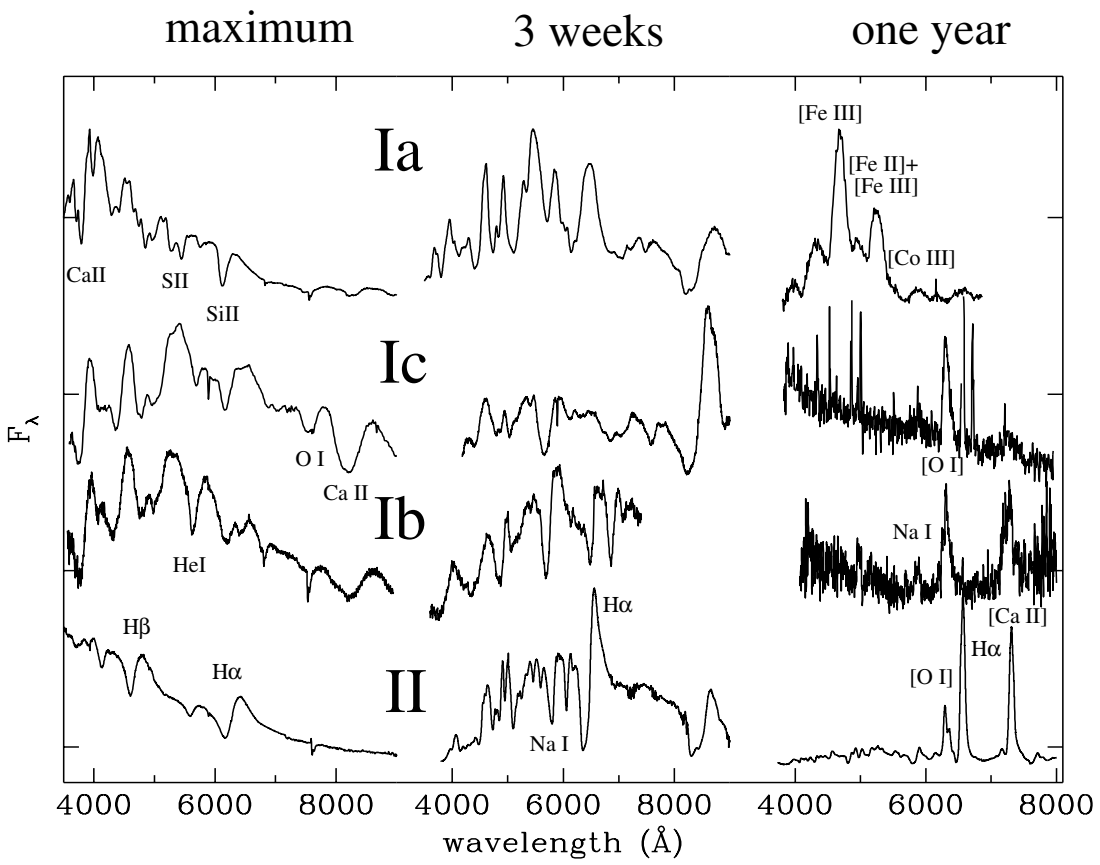

Figure 1.6 Spectral comparison from Turatto (2003)

1.3.2. Supernova rates

The observed supernova frequency carries important information about the underlying progenitor population. In this section we will concentrate more on SNe Ia-rates but will mention SNe II and SNe Ib/c where applicable.

Zwicky (1938) was the first work that tried to measure the supernova rate. By monitoring a large number of fields monthly, he arrived at a supernova rate by merely dividing the number of supernova detections by the amount of monitoring time and number of galaxies. This crude method resulted in a rate of one supernova per six centuries per galaxy.

Over time many improvements were made to this first method. Individual rates were calculated for different galaxy morphologies and different supernova types. To combine measurements from different galaxies the rate was normalised by dividing the supernova rate (measured by number of events per century) by galaxy luminosity (e.g. van den Bergh & Tammann, 1991; Tammann et al., 1994).

In recent years, however, rate measurements have been made in reference to mass and/or star formation, rather than just galaxy luminosity (SNe per century per 10^{10} $M_\odot$). The community (e.g. Mannucci et al., 2005) subsequently switched from B-Band photometry to the use of infrared photometry as the near infrared (NIR) is thought to better represent star-formation. B-Band photometry does not separate between mass and star formation (Hirashita et al., 2003).

Figure 1.10 plots the rate of supernovae per solar mass of material versus the galaxy mor-

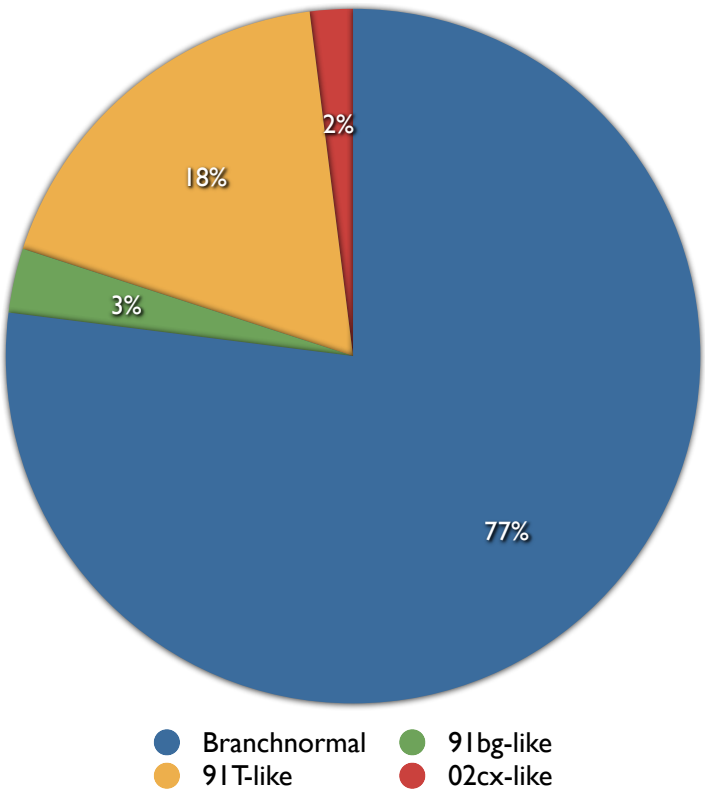

Figure 1.7 Estimated fractions for different Type Ia (SN Ia) classes for a purely magnitude limited search. Adapted from Li et al. (2011)

phology. The data clearly shows that there is a strong connection between morphology and supernova rates. For a long time it has been realised that SNe II and SNe Ib/c occurred preferentially in galaxies with active star formation, whereas SNe Ia occurred in all galaxy types. This indicates that SNe Ia and SNe II/Ib/c have different progenitors - with SNe II/Ib/c being related to young and presumably massive stars, and SNe Ia coming from a population of older stars. Theoretical calculations confirmed the view that stars larger than 8 $M_{\odot}$ should explode in a process known as core collapse (leading to SNe II/Ib/c), whereas white dwarf stars exceeding the Chandrasekhar mass ($M_{\rm Chan} = 1.38\,M_{\odot}$; Chandrasekhar, 1931) might explode as a SN Ia. The connection to massive stars was confirmed when the progenitor of SN 1987A was asserted as a massive star, along with the detection of neutrinos in line with theoretical predictions. The progenitors of SN Ia remains an open question, and a central topic of this thesis. Additionally, it seems the progenitors of SNe Ia occur in both young and old populations. This could hint that there are two main progenitor types, one which occur soon after star-formation, and another that takes a long time between formation and explosion.

To address this issue several groups have tried to measure a SNe Ia-rate that is completely independent of galaxy morphology (e.g. Mannucci et al., 2006; Maoz et al., 2010). This so-called, delay time distribution (DTD), measures the supernova rate over time following a brief outburst of star formation. This technique requires a detailed knowledge of the star-formation history of these systems. Several new techniques are emerging that try

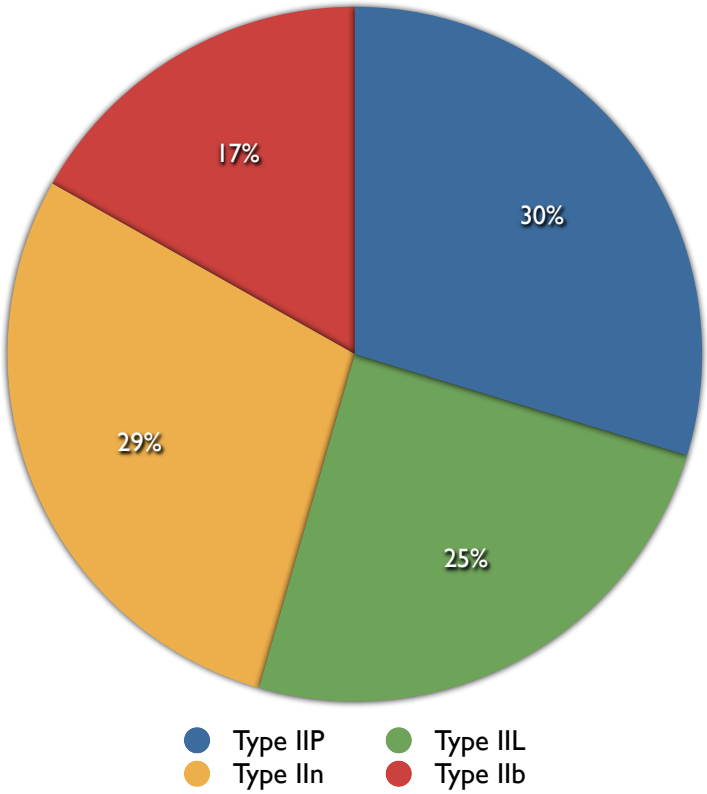

Figure 1.8 Estimated fractions for different Type II classes for a purely magnitude limited search. Adapted from Li et al. (2011)

to circumvent the intrinsically difficult task of determining star-formation for individual SNe Ia host galaxies (Maoz & Badenes, 2010; Barbary et al., 2010; Totani et al., 2008; Maoz et al., 2010).

Supernova rates and DTDs are an emerging tool to constrain progenitors. New upcoming surveys will provide an abundance of supernovae and measurements of their environments. However, fundamental uncertainties still exist on the theoretical front to predict DTDs for a given progenitor model.

1.3.3. Light Curves

Light curves give important insights into the physical processes occurring during the evolution of the supernova. Arnett (1982) for example deduced from the light-curve shape that Type I supernovae are eventually powered by the decaying ^{56}Co. For a brief overview of SN II light-curves we refer the reader back to Section 1.3.1.

For SNe Ia the light curve can be divided into four different phases (see Figure 1.11). In the first phase the SN Ia rises to the maximum brightness. Although only a small fraction of SNe Ia have been observed in the earliest parts of this phase, one can determine the time of the explosion by approximating the very early phase of a SN Ia with an expanding blackbody. The luminosity of this blackbody (in the Rayleigh-Jeans regime) is

$$L \propto v^2 (t + t_\mathrm{r})^2 T_\mathrm{eff}^4,$$

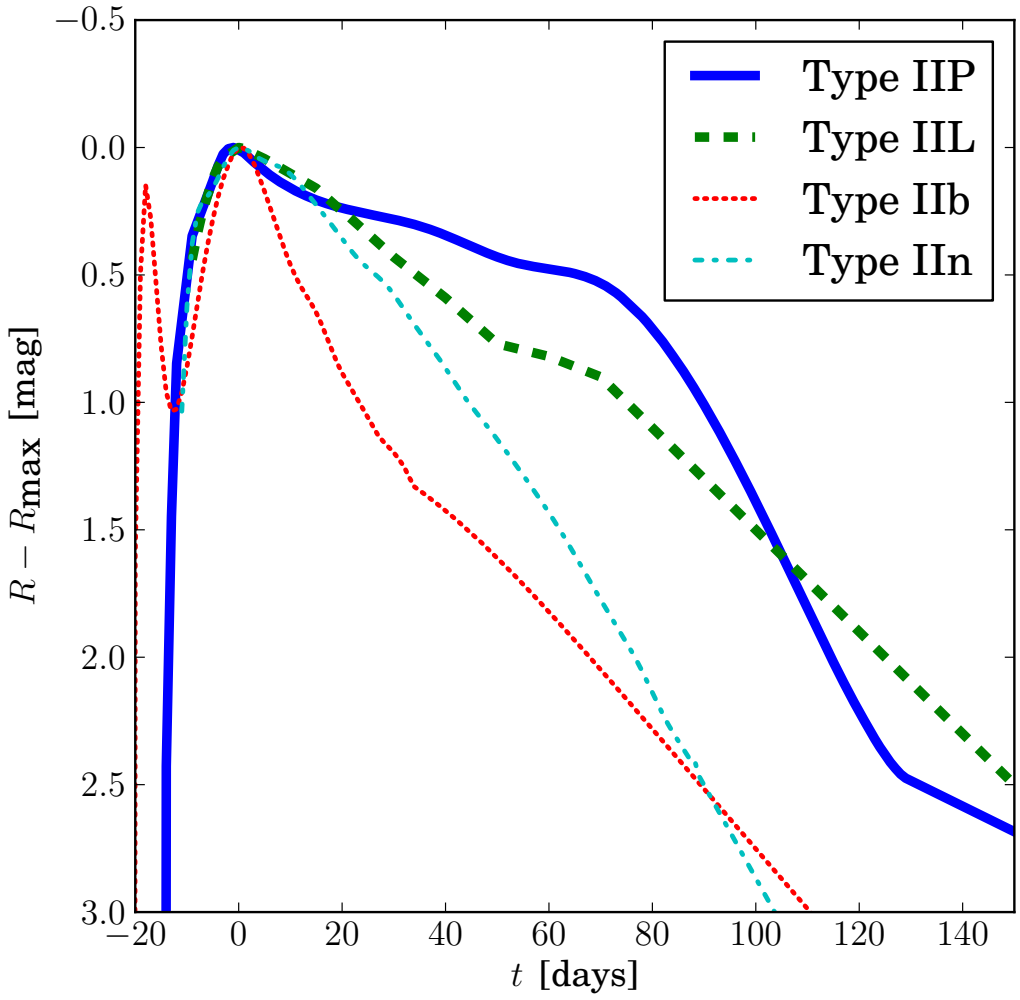

Figure 1.9 Light curve data taken from Li et al. (2011) templates. The time is relative to maximum light and the magnitude is the difference between maximum

where v is the photospheric velocity, T_{eff} is the temperature of the fireball, t is the time relative to the maximum and t_{r} is the rise time. The canonical rise time of SNe Ia is 19.5 days (Riess et al., 1999). New measurements using light curves of nearly four hundred SNe Ia, many these from the LOSS dataset, have however shown a shorter rise time (in B-Band) of 18 days (Ganeshalingam et al., 2011). The rise is very steep and the brightness increases by a factor of ≈ 1.5 per day until 10 days before maximum. In the second phase the SN Ia reaches the maximum first in the NIR roughly 5 days before the maximum in the B-Band (see Figure 1.11; Meikle, 2000). During the pre-maximum phase the colour stays fairly constant at $B - V \approx 0.1$, but changes non-monotonically to $B - V = 1.1$ thirty days after maximum. In the third phase SN Ia starts to fade but a second maximum is observed in the NIR (Wood-Vasey et al., 2008). Pinto & Eastman (2000) and later Kasen (2006) have successfully explained this by fluorescence of iron-peak elements in the NIR. Finally, in the last phase, light curves at late times can be used to probe the amount of ^{44}Ti

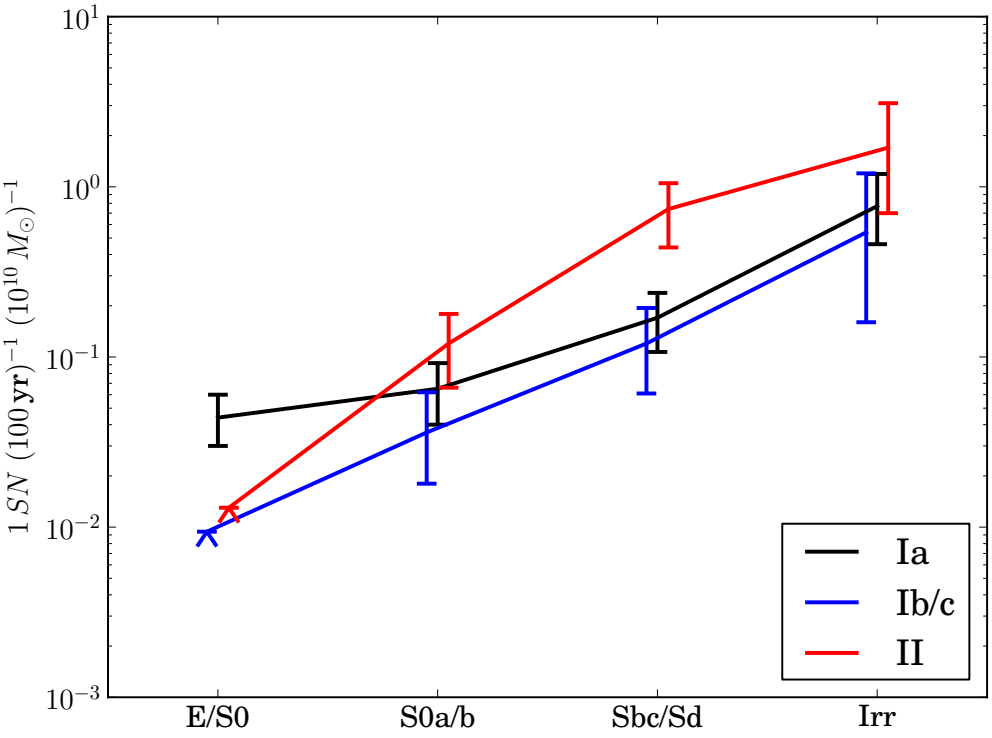

Figure 1.10 The plot shows the estimated supernova rate per unit mass in different galaxy morphologies (Mannucci et al., 2005). From left to right we plot old elliptical galaxies, lenticular galaxies, spiral galaxies and irregular galaxies. There have been no detections of SNe Ib/c and SNe II in old elliptical galaxies which suggests that these types only occur in galaxies with recent star-formation.

and other radioactive elements, but are complicated by light echoes (e.g. Schmidt et al., 1994b) and time dependent radiative transfer (Kozma et al., 2005). Leloudas et al. (2009) hold the record for the longest observed SNe Ia with SN 2003hv, which has been observed to nearly 800 days past maximum light.

1.3.4. Spectra

Spectra provide much more detailed information about supernovae than light curves. They are however, observationally much more expensive and difficult to precisely calibrate.

For all classes, supernova spectra can be divided into two phases: the photospheric phase and the nebular phase. In the photospheric phase, the spectrum can be very well approximated by a dense optically-thick core which has a black-body radiating surface with an optically thin expanding ejecta above. Photon creation is often negligible in the outer, optically-thin ejecta. The ejecta rather reprocesses the radiation field coming from the photosphere. In the case of SNe Ia this photosphere consists of layers of first intermediate mass elements (IMEs), and then IGEs, heated by the decay of ^{56}Ni. For SNe II the central region of the photosphere is hydrogen rich, which is kept hot by the energy deposited by the initial shock, diffusing outwards.

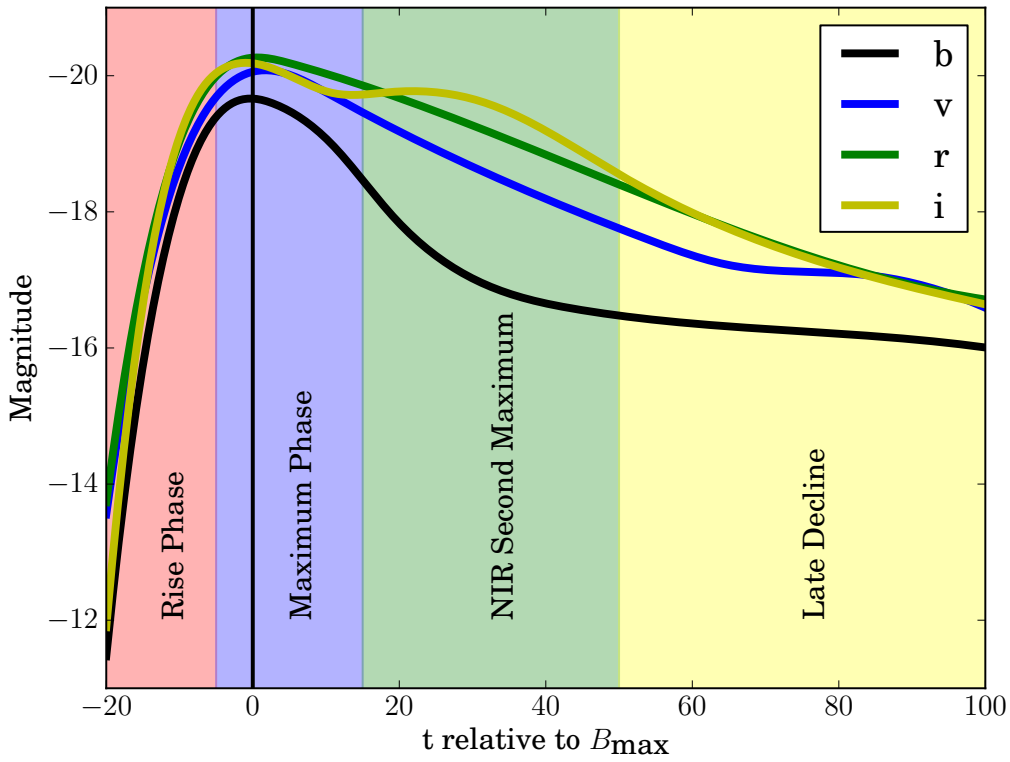

Figure 1.11 Light curves of SN 2002bo (data from Benetti et al., 2004)

As the supernova expands the photosphere recedes inward in mass and the optically thin layer grows larger and larger. Once sufficiently expanded, the entire SN ejecta becomes optically thin, which is known as the nebular phase. This phase is dominated by strong emission peaks and little continuum.

Type Ia supernova spectra

The time evolution of SNe Ia spectra is characterised by the photosphere shining through the ashes of the explosion. The inner core has nearly completely burned to IGEs, the shell above consists mostly of IMEs like sulphur and silicon. With the photosphere moving inward we first see IMEs before the photosphere goes deeper and deeper and shines through some of the core material. This onion-like structure can be probed by a method called supernova tomography. By modelling subsequent spectra one is able to reconstruct the individual shells of the supernova (Stehle et al., 2005; Hachinger et al., 2009). Modelling of SNe Ia spectra is an important part in understanding the explosion process of SNe Ia. Chapter **??** discusses this topic, which was explored in this thesis.

Similar to light-curves, the spectra have different phases. We will use the *Branch-normal* Type Ia, SN 2003du, to demonstrate the spectral evolution (Tanaka et al., 2011):

Pre-Maximum Phase In the pre-maximum phase the spectrum shows very high line velocities (up to 18,000 km s^{-1}) which measure the location of the photosphere in the

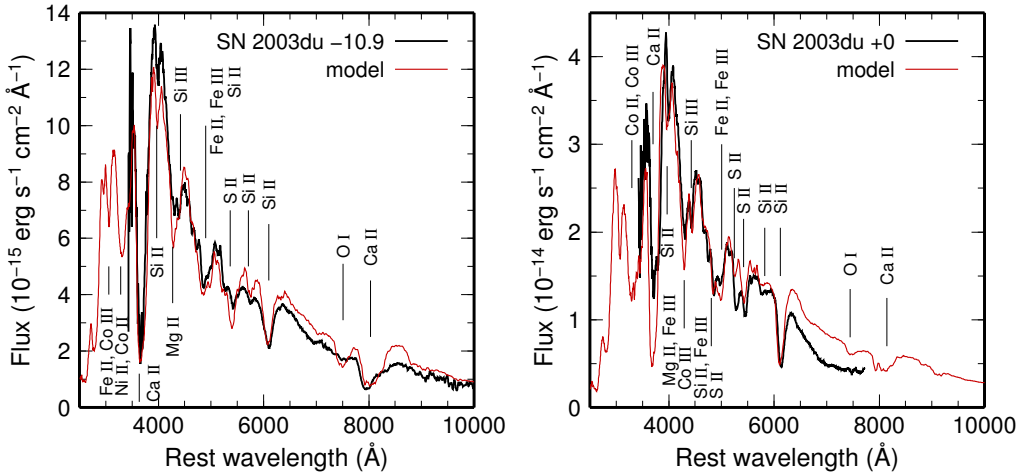

(a) SN 2003du ten days before maximum light The P Cygni-profiles of Silicon are clearly visible

(b) SN 2003du spectrum at maximum light. The light in the UV is being suppressed and fluoresced into the red part of the spectrum.

Figure 1.12 Pre-maximum evolution of SN 2003du (Figures kindly provided by M. Tanaka; Tanaka et al., 2011).

ejecta. There is a relatively well defined pseudo-continuum with strong P Cygni-profiles[1] of IMEs and IGEs (see Figure 1.12). The IGEs seen at this early phase are mostly primordial as the burning in the outer layers is incomplete and does not produce these elements.

The Ca II line is prominent in the blue and often shows extremely high velocities at early times (in SN 2003du $v_{\rm ph} \approx 25,000$ km s^{-1}). There have been multiple suggestions for the cause of this unusual velocity, including interaction with calcium in the CSM or high-velocity ejecta blobs (Hatano et al., 1999; Gerardy et al., 2004; Thomas et al., 2004; Mazzali et al., 2005; Quimby et al., 2006; Tanaka et al., 2006; Garavini et al., 2007). There is a strong Mg II feature at 4200 Å which is contaminated by several iron lines. Silicon and sulphur both have strong features at 5640 Å (S II) and at 6355 Å (Si II). While the strong silicon line at 6355 Å is the trademark of SNe Ia, the 'w' sulphur feature at 5640 Å cleanly separates SNe Ia from their SNe Ib/c cousins. It is believed that in these early phases one should be able to see carbon and oxygen from the unburned outer layers. There is the C II-feature at 6578 Å but it is normally very weak (if visible at all). The only strong oxygen feature is the O I triplet at 7774 Å. High temperatures that ionise a large amount of the oxygen as well as contamination by magnesium and silicon near the only oxygen line, often make it hard to constrain the abundance of oxygen well. Thus, large fractions of oxygen in the ejecta might not be a visible in SNe Ia spectra.

Maximum Phase As the supernova rises to the peak luminosity, opacity from the large fraction of IGEs (especially ^{56}Ni) is suppressing flux in the UV causing it to be reemitted in the optical/IR (see Figure 1.12). The photospheric velocity has now dropped to less than 10000 km s^{-1}. Nugent et al. (1995) suggested that at these epochs the ratio of Si II 5972 Å

[1] A profile which shows a emission peak at the rest wavelength of the line and a blue-shifted absorption trough

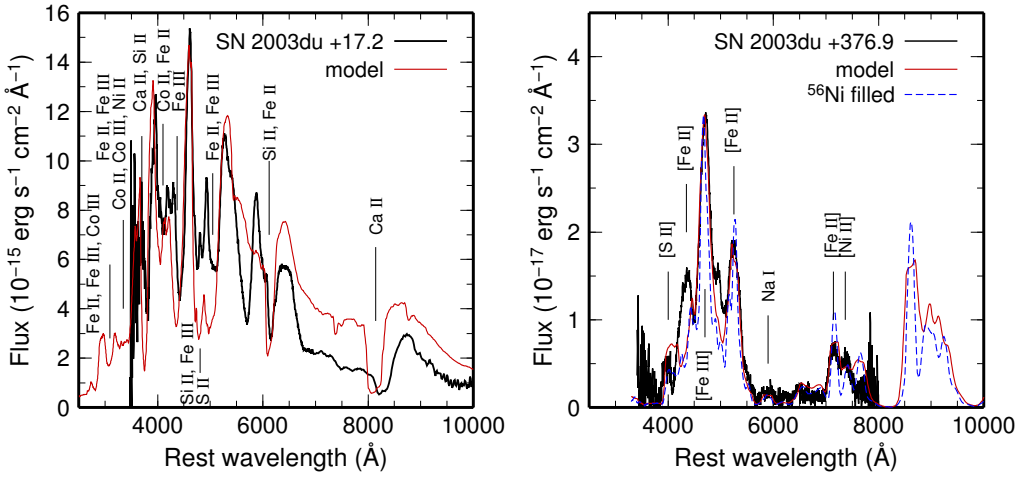

(a) SN 2003du 17 days past maximum light. The contribution of IGE is still rising.

(b) In the nebular phase strong emission lines are visible. This phase is not observed very often but contains crucial information about the explosion physics.

Figure 1.13 Post-maximum evolution of SN 2003du (Figures kindly provided by M. Tanaka; Tanaka et al., 2011).

and Si II 6355 Å is a good indicator for luminosity and can be an additional calibration tool for the absolute magnitude of individual SNe Ia.

Post-Maximum phase In the post maximum phase, the spectrum is increasingly being dominated by IGEs, as the photosphere has receded further into the ejecta. The photospheric velocity drops to less than 8000 km s^{-1}(see Figure 1.13). The spectrum continues to contain feature of IMEs, which are slowly overwhelmed by the IGEs.

Nebular-Phase As the supernova fades, the photosphere recedes into oblivion. At this stage the spectrum is characterised by strong emission lines which are produced by the IGEs from the very core of the explosion (see Figure 1.13). These are kept hot by the thermalisation of gamma rays and positrons from the radioactive decay of ^{56}Co, the daughter of ^{56}Ni. We are seeing into the slow moving ejecta with velocities under 5000 km s^{-1}.

Type II Supernova Spectra

SNe II show much more variation in spectra across their class than SNe Ia . In this section we will only give a very general and brief overview over SNe II spectra and spectral evolution. Compared to SNe Ia the initial spectrum is a relatively undisturbed continuum (see Figure 1.6). The only strong lines visible are those of hydrogen and helium which are the elements present in the envelopes of the progenitors. As the photosphere cools, the spectrum is broken up into P Cygni profiles of strong resonance lines of Ca II, Fe II, Na I, and elements like scandium in the envelope, which typically has near-solar composition. The nebular spectra of SNe II are characterised by hydrogen, oxygen and calcium emission lines powered by the radioactive decay of ^{56}Ni in the core of the supernova, which energises the

large amounts of hydrogen as well as the intermediate mass elements synthesised in the star before explosion.

1.3.5. X-Ray & Radio observations

Compared to preponderance of optical observations, X-ray and radio observations of supernovae are relatively rare. The information, however, carried in the very high and low frequency photons is invaluable to understanding various transient events.

One mechanism to produce X-ray and radio radiation is in shocks. When the expanding ejecta of supernovae hits the CSM, it produces synchrotron radiation in both wavebands. There have been extensive radio and X-ray observations of SNe II and SNe Ib/c that detail the mass-loss history of these massive stars. It is interesting to note that SNe Ia have never been detected in either X-ray or radio which suggests that the CSM around these objects is not very dense (for more detail see Section 1.5.3). Jets, and their interaction with the CSM, are another phenomenon commonly associated with radio emission. The GRB-phenomenon has been suggested to be the relativistic jet launched from certain SN Ib/c (e.g. Umeda & Yoshida, 2010). It is believed that GRBs are visible when this jet points towards the observer (also known as on-axis) within the opening angle of the jet thought to be about 5 degrees in the case of bright GRBs. As they evolve, a GRB's jet spreads and is thought, after many months, to emit isotropically at radio frequencies. This radio glow should be visible to both on-axis and off-axis observers. Soderberg et al. (2006) have started a campaign to find this isotropic radio emission and were rewarded when SN 2009bb showed radio emissions at late times (Soderberg et al., 2010). This signal was interpreted as relativistic outflow powered by a central engine and suggests an off-axis GRB.

SNe II/Ib/c have long been theorized to emit X-rays when the shocks from the collapsing core breaks out of the surface of the massive stars (Klein & Chevalier, 1978; Colgate, 1974). To observe these so-called shock breakouts is technically very challenging as the supernova needs to be detected very early. SN 2008D was serendipitously discovered during an observation with the Swift satellite's X-ray telescope. Swift was in the process of observing another supernova SN 2007uy in the same galaxy when it picked up an extremely luminous X-ray source (Soderberg et al., 2008). Subsequent ground based follow-up revealed a brightening optical counterpart which turned out to be a SN Ib/c. The X-ray-flash is attributed to the theorized shock breakout.

Finally late time X-ray observations also probe weak high energy emission lines of the decaying radioactive ash. These weak emission lines are only visible in late time spectra of very nearby supernovae so it comes as no surprise that they have only been observed in SN 1987A (Sunyaev et al., 1987; Dotani et al., 1987). Radio and X-ray observation of both kinds of supernovae are still in their infancy and will provide great help when solving the current mysteries surrounding all types of supernovae.

1.3.6. Supernova Cosmology

Early in the last century astronomers were trying to gauge our place in the universe. Hubble (1926) was the first to definitively demonstrate that many nebulae were objects like our own Milky Way. He used, among other methods, the known intrinsic luminosity (L_0) of Cepheid variables and determined the distance using the observed luminosity ($L/L_0 \propto 1/r^2$). In addition, Hubble found that galaxies that were further away had a higher

velocity away from the Milky Way than close galaxies (Hubble, 1929). He suggested that the universe was in a state of constant expansion. Since Cepheid distance measurements are only possible for very close-by galaxies, astronomers were feverishly searching for brighter more precise distance probes (also known as standard candles). The discovery that supernovae are distant objects Baade & Zwicky (1934) motivated many astronomers to try to use them as standard candles (Baade, 1938; van den Bergh, 1960; Kowal, 1968; Leibundgut & Tammann, 1990; Miller & Branch, 1990).

This work culminated, nearly 70 years after its first inception, in another paradigm changing discovery. The accelerating expansion of the universe was discovered by two teams (Riess et al., 1998; Perlmutter et al., 1999), using the same principal as Hubble used to discover the expansion of the universe. Over the past 13 years, the discovery of acceleration has been augmented by measurements of the CMB (e.g. WMAP7; Komatsu et al., 2011), large scale structure (e.g. Blake et al., 2011), and more supernovae (Astier et al., 2011, e.g.) to come up with the consensus flat,Λ - CDM model of the universe (e.g. Sullivan et al., 2011)

SN II Cosmology SNe IIP have been first suggested as cosmological probes by Kirshner & Kwan (1974) who showed that the Expanding Photosphere Method (EPM) could provide absolute distances to SNe II. Schmidt et al. (1994a) were able to measure SN II distances in the Hubble flow, and found $H_0 = 73$ km s^{-1}/Mpc^{-1}. They used sophisticated models to predict the emerging flux, and the absorption velocity of weak lines in the spectrum to estimate the photospheric velocity. SN IIP have also been used as relative distance indicators (Hamuy & Pinto, 2002), but are observationally expensive and not as accurate as SN Ia (15% error for SN II vs 7% error for SN Ia (Nugent et al., 2006)).

SN Ia Cosmology The story begins with Kowal (1968) plotting redshift of Type I supernova host galaxies against the luminosity distance implied by their peak magnitude (assuming a peak luminosity of $M_{\rm peak} = -18.59$). Although crude (scatter of 0.6 mag), Kowal's measurement clearly showed that more distant supernovae were at a higher redshift. Roughly fifteen years later, the broad class of Type I supernovae was divided into three distinct subclasses (Ia, Ib and Ic). In the late 1980's many authors started to realise that the class of SNe Ia was very homogeneous (Branch & Tammann, 1992, and references therein) making them remarkable distance probes. Around the same time a Danish team discovered the first very distant supernova at $z = 0.3$ (Norgaard-Nielsen et al., 1989), but gave up their search when it became clear that technology was not yet in place to efficiently make cosmological measurements with SN Ia. The SCP started to target high redshift ($z > 0.3$) fields to use distant supernovae to study the deceleration of the universe (little did they know). The smart and successful strategy of comparing observations taken shortly before and shortly after dark time meant that they could discover a 'batch' of supernovae at once and do follow-up observations (Perlmutter et al., 1995). This 'batch' mode was required to convince time allocation committees on large telescopes (only very large telescopes could study distant supernovae) to award time to this seemingly high risk project. The Calán/Tololo supernova survey (CTSS; Hamuy et al., 1993) started in the early 1990's and targeted only supernovae at low redshift ($0.01 < z < 0.1$). By 1995 they had produced 30 new light curves for SNe Ia measured with only CCD technology to unprecedented detail (Hamuy et al., 1995). Advances in standardising the SN Ia candle were made by

Phillips (1993). Phillips found that there was a tight correlation between the decline in luminosity and the peak magnitude of a SN Ia which made these objects unrivalled distance indicators. Convinced by the ability to calibrate SNe Ia (Phillips, 1993) and the ability to discover them at high redshift (Perlmutter et al., 1995) a group of astronomers founded the HZSNS. Then the developments started happening in rapid succession. Inspired by the method of calibrating peak luminosity with the decline of the supernova both SCP and HZSNS developed more precise ways to determine the intrinsic peak brightness. The HZSNS parametrised the shape of the light curve in different bands as a function of their peak magnitude. This Multicolor Light-Curve Shape method (MLCS; Riess et al., 1996) using many different bands was able to include measurements of dust extinction. The SCP team used a different method of stretching light curve templates in time to match the observations. Both methods were able to measure the distance of SNe Ia to a precision of $\approx 6\%$. Using these new tools both teams independently made the baffling discovery that the expanding universe was not decelerating but accelerating (Riess et al., 1998; Perlmutter et al., 1999). This revelation required a revision to the standard cosmological model where more than 70% of the Universe is made up of a form of matter called Dark Energy.

Over the past ten years the measurement of the universe's equation of state has become a prime driver of SNe Ia science. New light curve fitting tools try to implement more complex treatments of dust extinction and are still under active development (e.g. Jha et al., 2007; Guy et al., 2007). Recent work on NIR light curves (Kasen, 2006) suggests that the peak absolute luminosity is not influenced as much as optical light curves by the production of ^{56}Ni which depends on the unknown progenitor. Serendipitously the effect of dust extinction at these wavelength is also much less compared to optical bands. This has motivated some members of the community (e.g. Mandel et al., 2011) to use NIR to calibrate SNe Ia to standard candles.

1.3.7. Post-explosion observations of Supernovae

In most cases, for SNe Ia, SNe Ib/c and SNe II, the distance to the supernova is too large to make detailed studies of the remnants of these events in years post-explosion.

However, when supernovae happen in the nearest galaxies (or our own), we have the chance of detailed post-explosion follow-up. SN 1987A, which exploded in the nearby Large Magellanic Cloud (LMC), provided an ideal candidate for follow-up post-explosion. Observations confirmed that a previously observed blue super giant was not visible post-explosion (Walborn et al., 1989) confirming that this massive star was the progenitor of SN 1987A. It was the first time a progenitor was identified with this 'direct detection' method and since then many more progenitors have been unearthed post-mortem (for a review see Smartt, 2009).

Modern X-Ray space telescopes provide data of exquisite detail to study the remnants of supernovae. Hydrodynamic and non-equilibrium ionisation simulations of shocks from the supernova ejecta with the interstellar medium (ISM) can be used to measure temperature, elemental abundances and other parameters related to the state of the ejecta (Badenes et al., 2003; Sorokina et al., 2004; Badenes et al., 2005). This technique of modelling has been used to scrutinise ancient remnants. Kepler and Tycho remnants have been unambiguously identified using X-ray spectroscopy to be remnants of SNe Ia with the models even able to distinguish between different types of SN Ia models (Badenes et al., 2006; Reynolds et al., 2007). This field is still at its infancy and future coupling of three dimensional models

with X-ray observations will help understand the explosions mechanisms for both physical types of supernovae: thermonuclear explosions and core-collapse of massive stars.

Light-echoes are features that appear when light from a supernova scatters on dust in the ISM. This has been suggested by Zwicky (1940), but only advancements in imaging techniques as well as digital processing made it possible to detect these echoes. Rest et al. (2005) pioneered this technique and found several of these echoes in the LMC. Follow-up observations by Rest et al. (2008b) showed that it is possible to obtain a spectrum and identify the type of supernova with it. Krause et al. (2008) and Rest et al. (2008a) subsequently observed the light-echo of Tycho's supernova (SN 1572) and identified it as a *Branch-normal* SN Ia, confirming the previous X-ray modelling results. Future wide-field surveys will hopefully reveal many more of these light-echoes. Beyond classification, light-echoes can also be used for a three dimensional spectroscopic view of supernovae (demonstrated on the example of the Cas A remnant; see Rest et al., 2011).

Post-mortem observations of supernovae and their light-echoes, although only available for nearby events, provide us with unique insights into these events. Light echoes give us direct information about the explosion, but are only available for a few thousand years post-explosion. Radio and X-ray studies are possible for much older remnants. Maoz & Badenes (2010) have scrutinised remnants in the LMC and can reconstruct the supernova history for the last 20,000 years. Coupled with star formation history estimates they can infer a DTD.

1.4. Core-Collapse Supernova Theory

All SNe II and SNe Ib/c are believed to be powered by the collapse of the electron-degenerate iron cores of massive stars, as demonstrated by the direct detection of their progenitors on archival images in a number of cases (for a review see Smartt, 2009). For the iron core to form there had to be several prior stages of evolution.

1.4.1. Evolution of Massive Stars

To understand the state of the star shortly before the supernova explosion it is imperative to follow its evolution. For the topic of core-collapse we will concentrate on the nuclear physics of single massive star evolution. There is ample evidence that some SNe II and SNe Ib/c progenitors are influenced by binary evolution (Podsiadlowski et al., 1992), but this evolution is much more complex and is outside the scope of this work. In this context massive stars are stars bigger than 8 $M_{\odot}$, the minimum mass for a star that is believed to explode as a SN II. Like all stars, massive stars spend most of their lives on the main-sequence burning hydrogen. This happens via the carbon-nitrogen-oxygen cycle and its various side-channels (e.g $^{12}C(p,\gamma) \rightarrow^{13} N(e^{+}\nu) \rightarrow^{13} C(p,\gamma) \rightarrow^{14} N(p,\gamma) \rightarrow^{15} O(e^{+}\nu) \rightarrow^{15} N(p,\alpha) \rightarrow^{12}$ C). For a 20 $M_{\odot}$ star this phase lasts for 8.13 Myr (see Woosley et al., 2002).

As the star evolves it begins to ignite Helium which burns via the triple-α process to Carbon ($3\alpha \rightarrow^{12}$ C) and then to Oxygen ($^{12}C(\alpha,\gamma) \rightarrow^{16}$ O). Table 1 in Woosley et al. (2002) lists 1.17 Myr for this phase.

Due to neutrino losses the stellar evolution is qualitatively different after helium burning. A neutrino-mediated Kelvin-Helmholtz contraction of the carbon-oxygen core describes the advanced stages of nuclear burning in massive stars (Woosley et al., 2002). This contraction is occasionally delayed when the burning of new fuel sources counter-acts the neutrino losses. The star in the end is composited of a series of shells that burn the above fuel and deposit the ashes on the shell below (see Figure 1.14). There are four distinct burning stages. Their principal fuels are carbon, neon, oxygen, magnesium and silicon.

In the carbon burning stage, two ^{12}C nuclei are fused to a highly excited state of ^{24}Mg magnesium which then decays slowly to via three possible channels (see Equation 1.1) .

$$\begin{aligned} {}^{12}\mathrm{C} + {}^{12}\mathrm{C} \rightarrow {}^{24}\mathrm{Mg}^{*} &\rightarrow {}^{23}\mathrm{Mg} + \mathrm{n} \\ &\rightarrow {}^{20}\mathrm{Ne} + \alpha \\ &\rightarrow {}^{23}\mathrm{Na} + \mathrm{p} \end{aligned} \tag{1.1}$$

Although oxygen has a lower coulomb barrier, the next nucleus to burn after carbon is neon. This layer is composed of ^{16}O, ^{20}Ne and ^{24}Mg and burns neon with high-energy photons from the tail of the Planck distribution ($^{20}Ne(\gamma,\alpha)^{16}O$).

In the next shell there is a composition of mainly ^{23}O, ^{24}Mg and ^{28}Si. The bulk nucleosynthetic reaction is shown in Equation 1.2.

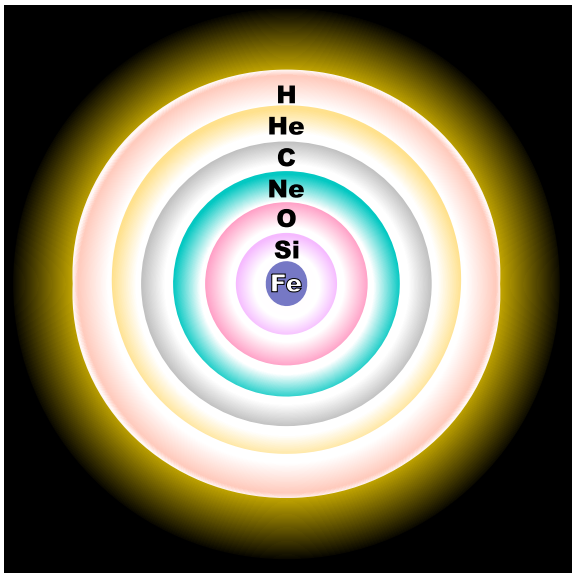

Figure 1.14 Shell Burning of a massive star before Type II. (Source Wikipedia)

$$
\begin{aligned}
{}^{16}O + {}^{16}O \rightarrow {}^{28}Si &\rightarrow {}^{31}S + n \\
&\rightarrow {}^{31}\mathrm{P} + \mathrm{p} \\
&\rightarrow {}^{30}\mathrm{P} + \mathrm{d} \\
&\rightarrow {}^{28}\mathrm{Si} + \alpha
\end{aligned}
\tag{1.2}
$$

The last shell converts ^{28}Si to IGE. The obvious reaction ^{28}Si +^{28} Si $\rightarrow^{56}$ Ni does not take place, but is replaced by a very complex network of isotopes that results in IGE being synthesised.

1.4.2. Core collapse

Before the collapse, the core consists of iron peak elements (see Figure 1.14). Neutrino losses during carbon and oxygen burning decreased the central entropy sufficiently so that the core becomes electron degenerate. Such a degenerate core, which is more massive than the Chandrasekhar mass (adjusted for Y_e, entropy, boundary pressure and other parameters) and with no material capable of being burned, will collapse.

There are two main instabilities that facilitate the collapse. As the density rises the Fermi-Energy becomes high enough for electrons to capture onto iron-group nuclei. This capture process removes electrons that were providing degeneracy pressure and reduces the structural adiabatic index. In addition, the temperature rises to values where the nuclear statistical equilibrium favours many free α-particles. The nuclear binding energy of this α-particle rich state is less and the core does not gain sufficient thermal energy to hinder gravity from advancing the collapse.

The collapse eventually leads to nuclear densities, the hard nuclear potential acts as a stiff spring during the compressive phase. It stores up energy and eventually releases this energy resulting in a *core bounce*. Recent simulations, however show that the ensuing

bounce shock is not sufficient for a SN II explosion with the shock loosing energy by photo disintegrating the nuclei it encounters (loosing roughly 10^{51} erg per 0.1 $M_{\odot}$).

The energy for a successful explosion is now thought to come from neutrino energy deposition. This reinvigorates the shock and leads eventually to an explosion which ejects the envelope of the massive star (Herant et al., 1994). Several variants of neutrino driven explosion now exist, with the neutrino driven convention leading to a Standing Accretion Shock Instability (SASI; Blondin & Mezzacappa, 2006), or acoustic g-mode oscillations (Burrows et al., 2007) . There is not yet a consensus on how stars more massive than 12 $M_{\odot}$actually explode. Regardless, in most cases for stars < 15 $M_{\odot}$, it is believed that a newly born neutron star is left behind in these explosions.

Woosley et al. (2002) provide a very comprehensive review of the theory of evolution and core collapse. In particular they go into more detail describing the scenarios after core-bounce.

1.4.3. Pair Instability Supernova

One alternate explosion scenario is the pair-instability supernova. This scenario is believed to only happen in stars with a helium core of more than 40 $M_{\odot}$. After core helium burning the star starts to contract at an accelerated rate, and enters a regime of temperature and density where the energy goes into electron-positron pair production rather than raising the temperature. This leads to a structural instability in the star (where the adiabatic index drops below ⅓), leading to collapse. This collapse, if significant densities are reached, will result in oxygen fusion, which eventually halts the implosion and the collapse turns into an explosion. For very high stellar masses, it is believed that oxygen fusion does not provide enough energy to halt the contraction and the star collapses to a black hole.

1.4.4. Type II Supernovae

After the collapse of the core, the supernova goes through three distinct phases. The observables of these stellar cataclysms are the light curve, spectra and for one case (SN 1987A), even the neutrino wind.

The shock-waves generated by the collapsing core reaching the surface, is the first visible signal from the supernova. Ensman & Burrows (1992) calculated a duration for the so-called shock breakout of SN 1987A to 180 s, its luminosity of 5×10^{44}erg s^{-1}. Such a breakout thus far has been observed only once - in the case of the lucky observations of SN 2008D - a SN Ib/c (Soderberg et al., 2008). This star, more compact than SN 1987A, had a shock breakout of 400 s with a luminosity of 6.1×10^{43}erg s^{-1}.

Secondly Shocks in the ejecta and the decay of ^{56}Ni irradiate the expanding hydrogen envelope and the energy slowly diffuses out causing a plateau, for the SNe IIP. SN IIL have lost most of their extensive hydrogen envelopes and radiate their energy much more quickly - resulting in the observation of a linear decline, rather than a plateau. The last phase begins after the photosphere moves through the entirety of the H envelope, the ejecta transform to become optically thin, the supernova suddenly drops in brightness, and then fades exponentially, following the 77 day half life of ^{56}Co, the daughter nucleus of ^{56}Ni. Some light might also be produced by shock interaction with the CSM.

1.4.5. Type Ib/c Supernovae

In the case of a SN Ib/c, the progenitor has lost at least all of its hydrogen envelope prior to core-collapse. This loss of envelope is presumed to be caused by stellar winds and/or binary interactions (Podsiadlowski et al., 1992). Thus the hydrogen can not provide a energy buffer and no plateau is visible, similar to a SN IIL. Instead the light-curve is powered by radioactive decay after shock breakout, with the energy diffusing out from the core. The missing envelope also causes the lack of hydrogen lines in the spectrum leading to the supernova being classified as Type Ib. If both hydrogen and helium envelopes are lost then the supernova is classified as Type Ic. .

1.5. Thermonuclear Supernova Theory

In this section we will discuss the theory of SNe Ia which are thought to be thermonuclear explosions of degenerate carbon/oxygen matter. The different progenitor scenarios leading to an explosion of a massive white dwarfs are discussed in Section 1.5.1.

1.5.1. Progenitors of Type Ia Supernovae

There are two basic scenarios for SNe Ia progenitors. The single degenerate scenario (SD-scenario) has a white dwarf accreting from a non-degenerate companion until the white dwarf ignites leaving behind the companion star (first introduced by Whelan & Iben, 1973). In the second scenario, the double degenerate scenario (DD-scenario), two white dwarfs merge and ignite, leaving no stellar remnant behind (first suggested by Webbink, 1984; Iben & Tutukov, 1984).

Single Degenerate Scenario

The SD-Scenario assumes a binary system with one evolved white dwarf and one non-degenerate companion. In most cases this non-degenerate companion is thought to be a main sequence to red giant star. There are also scenarios that involve 'exotic' companions such as helium stars. In most cases, the companion (or donor) star is believed to have filled its Roche-Lobe and lose mass via Roche Lobe Overflow (RLOF).

An outstanding problem of the SD-Scenario is the accretion process. As most white dwarfs are born with masses significantly less than the Chandrasekhar mass, they need to accrete mass to reach the critical 1.38 $M_{\odot}$. The accretion process needs to efficiently burn any accreted hydrogen into helium and subsequently to carbon/oxygen to explain its absence in SNe Ia spectra, and to prevent recurrent novae from removing material from the system. Theoretically, there is only a very narrow range of accretion rates that allows the white dwarf to accrete hydrogen, stably burn it and efficiently grow to the Chandrasekhar mass. Yoon & Langer (2004) have suggest that rotation of the accreting white dwarfs might increase this very narrow parameter range.

If the mass-accretion rate is too low, it causes nova explosions which are thought to eject more mass than the accretion prior has gained (Nomoto, 1982). However, there are some systems (e.g. RS Ophiuci, U Scorpii) that have white dwarf masses close to 1.4 $M_{\odot}$ which undergo recurrent nova outbursts. It is very likely that these systems were not born with a white dwarf this massive, but that these white dwarfs have successfully grown

in mass through the accretion of material. This suggest that in some cases, despite nova outbursts, efficient accretion is possible. Too high accretion rates would cause the binary to be engulfed in an extended red giant envelope. The debris of such an envelope are not seen in most SN Ia explosions - an exception might SN 2002ic.

There are several possible identified progenitor systems. A class of binaries called supersoft X-ray sources has a white dwarf accreting hydrogen from a non-degenerate companion at an appropriate rate such that hydrogen and helium burn hydrostatically. In cases where the white dwarf (WD) is a carbon/oxygen White Dwarf (CO-WD), rather than a oxygen/neon White Dwarf (ONe-WD), these objects are strong contenders for SN Ia progenitors (Di Stefano et al., 2006, and references therein). Another subclass of possible SD-Scenario progenitors are AM CVn stars (Nelemans, 2005). In this type of cataclysmic variable, material is accreted onto the WD from a helium star or helium WD (van den Heuvel et al., 1992). This scenario would conveniently explain the lack of hydrogen in SN Ia explosions . A SN Ia explosion in such systems is discussed in Section 1.5.2 on page 31.

Donor Stars

The SD-Scenario requires a secondary companion star (also known as donor star). If this companion survives the explosion it would be a calling card for the SD-Scenario. One consequence of this explosion is an unusual spatial velocity of the companion post-explosion. The main fraction of this velocity stems from the gravitational unbinding whereas only a small amount would originate in the kick from the supernova ejecta (see Figure 1.15; Canal et al., 2001; Han, 2008). Marietta et al. (2000) have simulated the impact of SN Ia ejecta on a main-sequence, sub-giant and red-giant companion. In the case of the main-sequence companion, the supernova ejecta heats a small fraction (1-2%) of the envelope which is lost post-explosion. Pakmor et al. (2008) have repeated the simulations for the main-sequence companion and find similar results, but suggest that even less mass is lost. Post-explosion the main-sequence star should be very luminous (500 – 5000 $L_{\odot}$) and is expected to cool down over next 1000 – 10,000 years and follow the main-sequence track (Marietta et al., 2000).

For the sub-giant companion the simulations show very similar results to the main-sequence companion. The sub giant looses only a small fraction of the envelope (10 – 15%) and like the main-sequence star, it will be very luminous shortly after the explosion. After thermal equilibrium is established, the companion will return to a post-main-sequence track.

The case of the red-giant, however, is different. Marietta et al. (2000) suggest that it will lose most of its loosely bound envelope. Post-explosion core contracts and the temperature rises to more than 3×10^4 K. The object may appear as an under luminous main-sequence O or B star. Justham et al. (2009) have suggested the population of low-mass single white dwarfs to be the remaining cores of such red-giant donor stars. This would result in a convenient explanation for the existence of these objects.

One feature of surviving companions may be an unusually large rotational velocity post-explosion (Kerzendorf et al., 2009, Chapter **??** of this work). Due to tidal coupling during the RLOF phase, the rotational velocity of the donor star, post explosion, is directly tied to the binary rotational velocity (see Figure 1.16). Since stars of F spectral-type and later do not display such high rotational velocities, this feature is a very useful discriminant

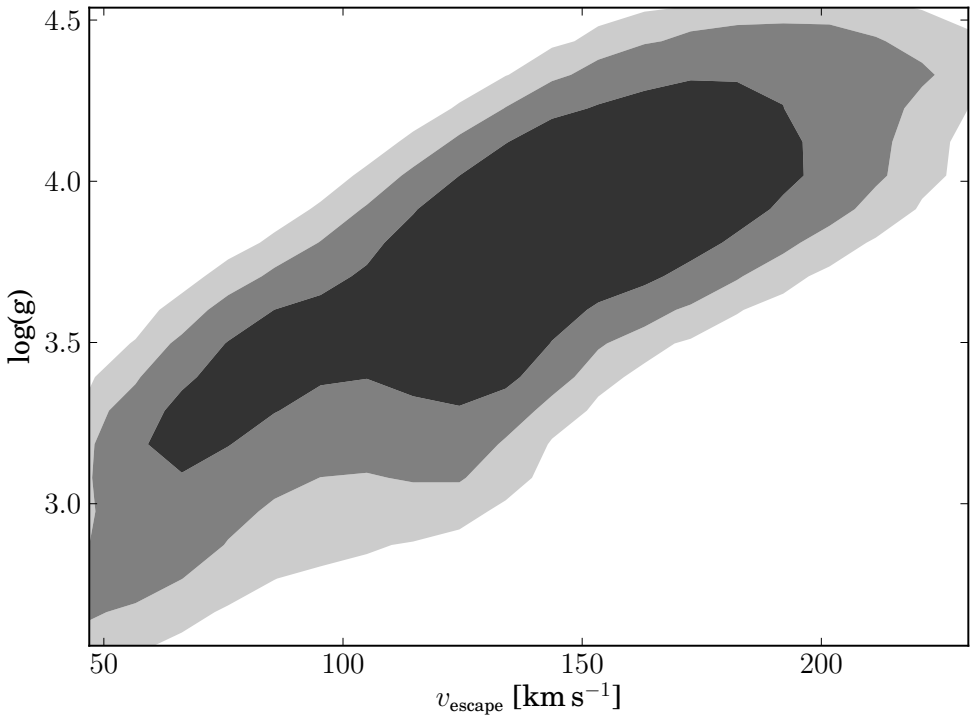

Figure 1.15 Expected escape velocity for different evolutionary states of the donor star based on binary population synthesis (Han, 2008, data kindly provided by Z. Han)

when looking for donor stars.

There have been several attempts to find these objects in ancient supernova remnants. Schweizer & Middleditch (1980) found a OB subdwarf star located 2.5′ from the centre of the remnant of SN 1006 and suggested this as the donor star. Subsequent analysis by Wu et al. (1997, 1983) however, have revealed strong Fe II features with a profile broadened by a few thousand km s^{-1}and ionised redshifted silicon features. In the very likely case that these features are caused by the remnant this indicates the star to be located behind the remnant rather than being involved in the SN Ia explosion as a donor star.

The search for donor stars in ancient remnants is one of the main parts of this thesis and we direct the reader to Chapter **??** through Chapter **??**.

Double Degenerate Scenario

Webbink (1984) and Iben & Tutukov (1984) were the first to suggest merging white dwarfs as progenitors for SN Ia. There are several advantages to the DD-Scenario. For example, it naturally explains the lack of hydrogen in SN Ia spectra. The accretion problem encountered in the SD-Scenario is dispensed with in the DD-Scenario, as long as the sum of masses of both CO-WD's is above Chandrasekhar mass - although new ideas might make this an upper limit rather than a requirement (van Kerkwijk et al., 2010).

One problem with this scenario, however, is that most SN Ia form a relatively homogeneous class. It is hard to reconcile this fact with the merger of two white dwarfs with

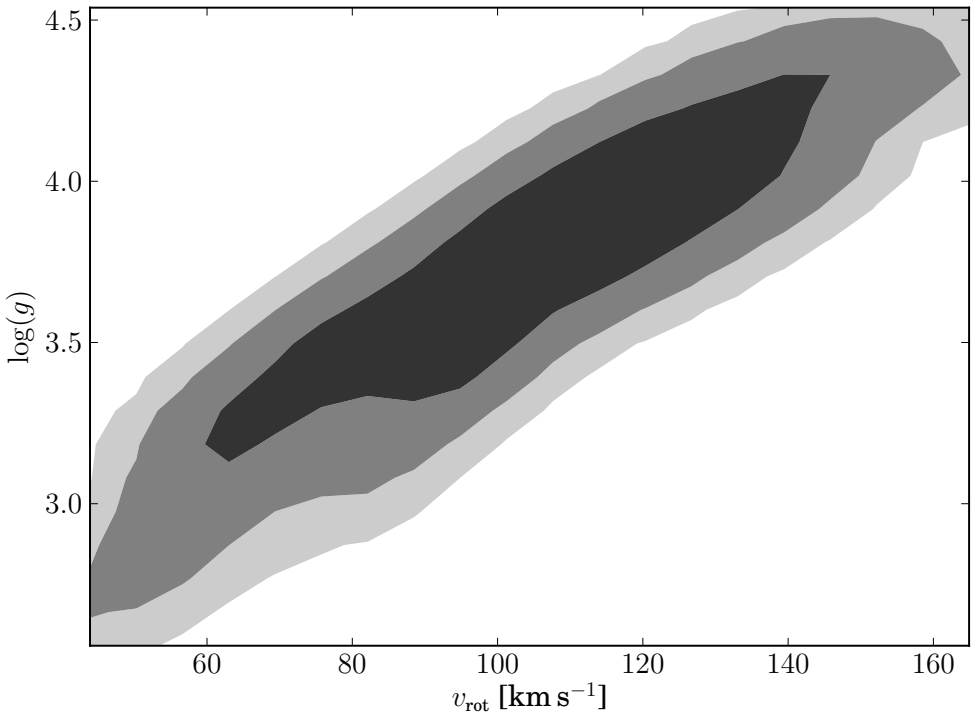

Figure 1.16 Expected rotational velocity for different evolutionary states of the donor star post-explosion based on binary population synthesis (Han, 2008, data kindly provided by Z. Han)

different initial masses, composition, angular momenta and different impact parameters. A potentially even larger problem, however, is that the accretion of the disrupted lighter white dwarf onto the more massive white dwarf is thought to lead to accretion induced collapse (AIC) rather than a thermonuclear explosion (see Section 1.5.2).

Pakmor et al. (2010) have simulated the merger of two equal-mass white dwarfs (0.9 $M_{\odot}$) and conclude that the outcomes of these mergers might be subluminous SNe Ia.

In summary, mergers of white dwarfs might be able to explain some of the SN Ia class. It is however still debated if these events are responsible for the abundance *Branch-normal* SNe Ia.

1.5.2. Evolution and Explosion of Type Ia Supernovae

White Dwarfs

CO-WDs are thought to be the progenitor stars of SNe Ia. White dwarfs are among the most common stellar objects that are not composed primarily of hydrogen, which is consistent with the lack of hydrogen in SN Ia spectra. Furthermore, there is a clear theoretical avenue to exploding white dwarf stars, through accretion of material to near the Chandrasekhar mass. It is general believed that these objects accrete matter (for the possible scenarios see section 1.5.1) until they get close to the Chandrasekhar mass. It is a delicate balance between conditions for ignition that results in a thermonuclear run-away

and reaching the Chandrasekhar mass threshold, which would lead the collapse of the star to a neutron star.

There are three main classes of white dwarfs: helium WDs, CO-WDs and ONe-WDs. Originally ONe-WDs were called ONeMg WDs but the mass fraction of magnesium had been overestimated and thus now only oxygen and neon are mentioned (Ritossa et al., 1996).

The accretion onto a helium WD would lead to helium burning well before the Chandrasekhar mass and thus these objects are not considered as potential progenitors. Although not considered as the SN Ia progenitor itself helium, WDs as companions to CO-WDs are an interesting suggestion as SN Ia progenitor systems (see Section 1.5.2). The ultimate fate of an accreting ONe-WD is thought to be the collapse into a neutron star. Theoretical models predict that before oxygen can be ignited, electron capture begins in the core ($^{20}\mathrm{Ne}(e^-,\nu)^{20}\mathrm{F}(e^-,\nu)^{20}\mathrm{O}$). Heating by the resulting γ-rays starts explosive oxygen burning. However, the electron-capture is much faster than the oxygen burning and promotes the collapse to a neutron star (Nomoto & Kondo, 1991; Gutiérrez et al., 2005).

The favoured progenitor for a SN Ia are CO-WDs. Theoretical calculations predict that these objects ignite when very close to the Chandrasekhar mass (1.38 $M_\odot$). The vast majority of white dwarfs are born with masses around 0.6 $M_\odot$ (Kepler et al., 2007) due to the large abundance of $\approx 1\ M_\odot$ stars compared to stars with a mass $> 5\ M_\odot$ which would turn into more massive WDs. It is, however, quite frequent to have WD stars built up to more than 1 $M_\odot$ through mass transfer in binary systems with an intermediate mass companion ($2\ M_\odot < M < 8\ M_\odot$) . Such systems are thought to be the eventual progenitors of SN Ia.

Pre-Supernova Evolution

The white dwarf gradually accretes more and more material. Close to Chandrasekhar mass mild carbon burning ensues

$$\begin{aligned} {}^{12}\mathrm{C}({}^{12}\mathrm{C},p) &\rightarrow {}^{23}\mathrm{Na} \\ {}^{12}\mathrm{C}({}^{12}\mathrm{C},\alpha) &\rightarrow {}^{20}\mathrm{Ne} \\ {}^{12}\mathrm{C}({}^{12}\mathrm{C},n) &\rightarrow {}^{23}\mathrm{Mg}, \end{aligned} \tag{1.3}$$

but is mediated by photon and neutrino losses (Lesaffre et al., 2005; Iliadis, 2007). As these cooling processes become less effective convection starts in the core and the energy output in the core increases. At this stage the thermal structure is largely controlled by what is termed *Urca* pairs. These reaction pairs consist of alternating electron captures and β^- decays involving the same pair of parent and daughter nuclei. Two prominent examples which are important in pre-supernova evolution are $^{21}\mathrm{Ne}/^{21}\mathrm{F}$:

$$\begin{aligned} {}^{21}\mathrm{Ne}(e^-,\nu) &\rightarrow {}^{21}\mathrm{F} \\ {}^{21}\mathrm{F}(\beta^-\nu) &\rightarrow {}^{21}\mathrm{Ne} \end{aligned} \tag{1.4}$$

These processes can lead to either cooling or heating (Lesaffre et al., 2005).

At present, the pre-supernova evolution has proven difficult to model theoretically as it is likely to be non-local, time-dependent, three-dimensional and stretches over hundreds of years. The exact conditions at the time of explosion are therefore poorly constrained,

and all explosion models have to assume simple initial conditions. The main steps leading to the explosion follow.

Explosion mechanisms

Ignition The *Urca* processes will dominate core evolution for the last thousand years until explosion. As the temperature rises to $T \approx 7 \times 10^8$ K (Hillebrandt & Niemeyer, 2000) the convection time (τ_c) increases and becomes comparable to the burning time (τ_b). Consequently the convective plumes burn as they circulate. Once the temperature reaches $T \approx 10^9$ K, τ_b becomes very small compared to τ_c and carbon and oxygen largely burn in place. This is the moment of ignition. As the convective plumes burn while they rise it is likely that the initial flame seed does not start in the centre of the core. Röpke & Hillebrandt (2005) have used multiple flame seeds in their three dimensional full star models.

Thermonuclear Explosion After ignition, there has historically been two main options. The first option was the complete detonation (supersonic flame front) of the CO-WD (Arnett, 1969). It was quickly, discovered, however that this method burns the entire star to nuclear statistical equilibrium (NSE) (^{56}Ni dominant), and thus leaves none of the IMEs observed in SNe Ia.

To counteract this problem, it was suspected that the star instead of detonating would deflagrate (subsonic flame wave, mediated by thermal conduction). The fuel in front of the deflagration becomes rarefied by the energy from the flame, with hot light burning bubbles rising into the cold dense fuel creating Rayleigh-Taylor instabilities (see Figure 1.17 at t=0.72 s). Detailed calculations show that once the deflagration wave has run through the star, the resulting production of ^{56}Ni is lower than that observed in SNe Ia. More critically IMEs are left throughout the expanding debris, leading to an un-observed distribution of IMEs at low velocities (Mazzali et al., 2007).

The currently favoured scenario is the one of delayed detonation. Here, the star initially burns like in the deflagration scenario with the inhomogeneities in the deflagration front producing hot spots. We refer the reader to Schmidt et al. (2010) and references therein, for a detailed explanation of the transition from a deflagration to a detonation wave. Once the detonation wave has formed it travels through the unburned star - not penetrating the already deflagrated nuclear ashes. This produces an event which observationally is a good match to the spectral evolution of SNe Ia (e.g. Kasen et al., 2009). Figure 1.17 shows clearly how the detonation wave wraps around the cold ashes over the course of the detonation. An open question is if and how these transitions from deflagration to detonation occur in SNe Ia.

Sub Chandrasekhar Mass detonations Livne (1990), Shigeyama et al. (1992), Livne & Arnett (1995) and Sim et al. (2010) have explored the detonation of CO-WDs at sub Chandrasekhar Masses. Sim et al. (2010) show that the detonation of a sub Chandrasekhar mass CO-WD reproduce observed light-curves and early-time spectra of SNe Ia fairly well.

A significant issue in this scenario is the ignition. Fink et al. (2010) have studied an explosion mechanism in which a surface detonation of a helium shell drives a shock-wave into the core. In the core this shock wave triggers an ignition by compression. As an initial model they use a CO-WD accreting from a helium rich companion building a thin helium

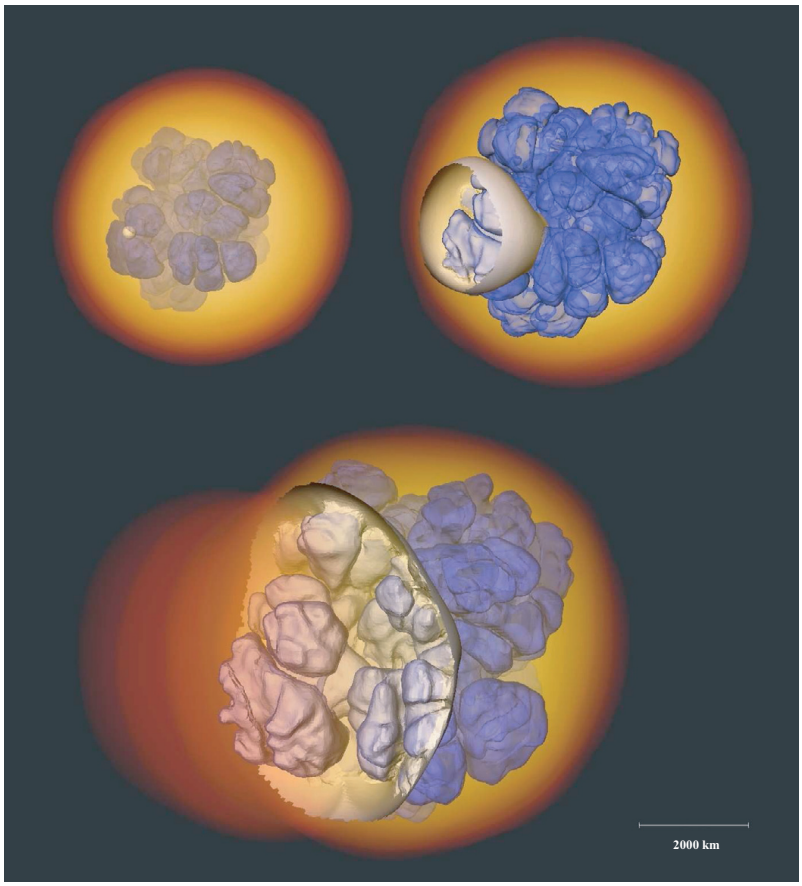

Figure 1.17 Delayed detonation simulation from Röpke & Bruckschen (2008). The upper panels show the deflagrated interior (marked in blue) and the detonation ignition point (small white sphere). The detonation wave wraps around the deflagration ash and consumes the cold fuel. (Image reproduced with kind permission of Fritz Röpke)

shell around its CO interior (described in Bildsten et al., 2007). This helium shell is ignited and sends out a shock wave. As the helium flame spreads in the shell around the star it sends a shock wave into the core. Once the shock waves converge off-centre they create an environment hot and dense enough that the ignition of a detonation wave may be possible (see Figure 1.18.)

This scenario reproduces the intrinsic luminosity variability in the class of SN Ia as each exploding white dwarf can have a different mass, but might predict too much variation.

Super Chandrasekhar Mass Detonations As well as sub Chandrasekhar mass explosions, the community has also studied the explosion of white dwarfs with $M > M_{\mathrm{Chan}}$. There have been a small number of SNe Ia which were extremely luminous (e.g. SN 2003fg, SN 2006gz, SN 2007if and SN 2009dc) suggesting ejecta masses of much more than 1.4 $M_{\odot}$(Howell et al., 2006; Hicken et al., 2007; Yamanaka et al., 2009; Scalzo et al., 2010; Tanaka et al., 2010; Silverman et al., 2011; Taubenberger et al., 2011). This raises the question why these objects do not undergo AIC. Yoon & Langer (2005) suggest that through rapid rotation these objects will increase the effective Chandrasekhar mass. Another possibility is the merger of two massive white dwarfs. Pakmor et al. (2010) however suggested, for the merging of equal-mass 0.9 $M_{\odot}$ CO-WDs (a total mass of 1.8 $M_{\odot}$), the resulting supernova

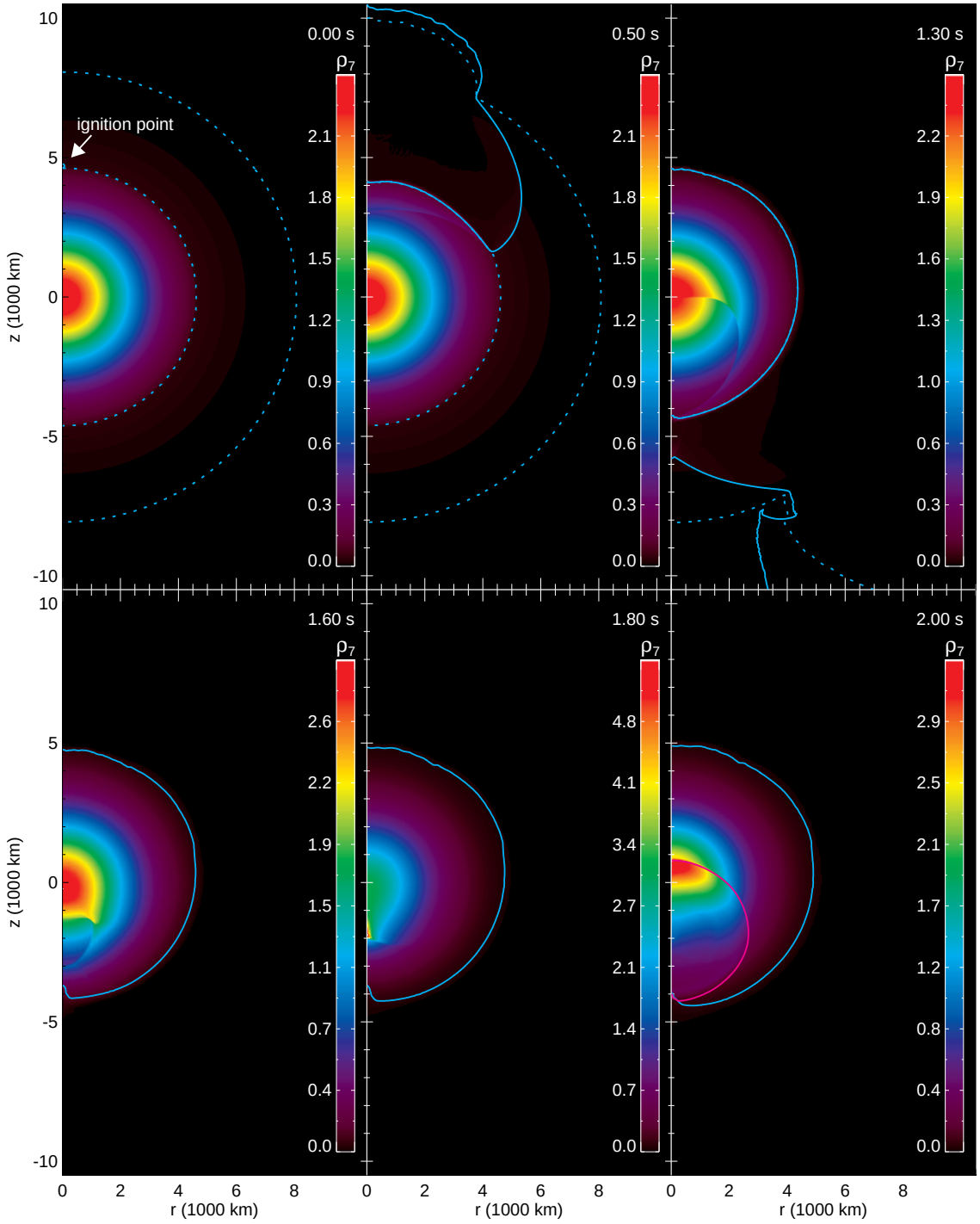

Figure 1.18 The ignition point of the helium shell is marked in the upper left image. We can follow the helium shell sending shock waves into the core of the white dwarf. They converge in the lower left image at the opposite site of the Carbon/Oxygen core (data from Fink et al., 2010, Figure kindly provided by Michael Fink).

would resemble the class of 91bg-like objects. A core collapse scenario for some of these events has also been constructed. The number of observed super Chandrasekhar mass supernovae is as of yet too low to define common characteristics or a class.

1.5.3. Constrains for different progenitor scenarios

The question of the progenitors of SNe Ia is a main part of this thesis and one of the most highly debated subjected in current SNe Ia research. There are various arguments for and against the SD-Scenario and the DD-Scenario, with some suggesting that both scenarios contribute to the class of *Branch-normal* SNe Ia.

Patat et al. (2007) have found a variable blue-shifted sodium absorption feature using high-resolution spectra of SNe Ia. This suggests that there is sodium rich material in the line-of-sight. The variability suggests that this material is close to the supernova explosion. One explanation of this variability is the change in the ionisation state of the sodium atoms in a nearby CSM caused by the variable SN Ia radiation field. Very recently a study by Sternberg et al. (2011) observed sodium features in 30 SNe Ia. They found that many of these SNe Ia show blue-shifted sodium features relative to the host galaxies rest frame, which can be explained by expanding winds from the progenitor system. Finally, Patat et al. (2011) have seen similar features in the recurrent nova RS Ophiuci. This could hint that recurrent novae with red giant donor stars might be responsible for some SNe Ia.

Di Stefano (2010) have not found enough supersoft X-ray source to account for the rate of SNe Ia. In addition, Gilfanov & Bogdán (2010) have not found enough accumulated X-ray flux from elliptical galaxies if all SN Ia progenitors were supersoft X-ray source (assuming the X-Ray flux calculated for these objects is correct). The main caveats here are that the SN Ia-progenitors might only be in the supersoft X-ray source phase for a short amount of time and at other times, these objects could be engulfed in a envelope, which would reprocess the produced X-rays to optical or infrared wavelengths. In stark contrast to the negative X-ray studies described above, Voss & Nelemans (2008) have suggested that they found the progenitor of the Type Ia SN 2007on in X-rays. Further analysis has put this claim in doubt (Roelofs et al., 2008). Although the detection might have been spurious, their technique remains promising: Following up SNe Ia in X-ray-archives could detect potential SNe Ia progenitors in a pre-explosion X-ray phase and could confirm the supersoft X-ray source scenario for some SNe Ia.

It remains a mystery that SNe Ia do not show lines of hydrogen which might be expected from the wind or stripped envelope in the SD-Scenario. Leonard (2007) have searched in the nebular spectra of two SNe Ia for hydrogen and place an upper limit of 0.1 $M_{\odot}$ for both these explosions. On the other hand, Justham (2011) suggest that a red giant donor could significantly shrink during the RLOF and the material stripped by the ejecta might be negligible. This would place the the stripped hydrogen below the current detection limit.

Kasen (2010) predicts excess in ultra violet (UV) flux in the SN Ia light curve at early times for SN Ia from single degenerate systems. This effect depends on orientation of the system to the line of sight and the state of the donor. The effect would be biggest for a red giant donor star. Hayden et al. (2010) do not see this excess in the SDSS supernova set indicating that the red giant channel is not common for SNe Ia. A study by Bianco et al. (2011) using the SNLS data set comes to the same conclusion. To conclusively state a lack of this predicted excess a big sample of very early light curves is needed, which does not exist yet.

Radio observations in the case of SNe Ia can, for example, reveal the shock interaction of the ejecta with the CSM. The SD-Scenario predicts a more dense CSM than the double degenerate scenario. Hancock et al. (2011) have stacked radio observations of SNe Ia

in the visibility plane and have not detected any source. At present, it is not clear that this limit is in conflict with the SD-Scenario. Future stacked Extended Very Large Array (EVLA) measurements will push the limits substantially down and will hopefully provide constraints that will allow us to rule out one or the other scenario, at least for some SNe Ia.

Finding a donor star of the SD-Scenario in a supernova remnant (SNR) post-explosion would resolve the question for the progenitor system, at least in the searched remnants. The main work of this thesis investigates this technique and we will refer the reader to Chapter **??** through **??**.

Population synthesis together with observations of DTDs are an important step in exploring the different progenitor scenarios. Hachisu et al. (2008); Han & Podsiadlowski (2004) have explored the SD-Scenario parameter space and suggest, when compared to observations, that the SD-Scenario can almost explain the observed DTD (for references on DTD see section 1.3.2). Ruiter et al. (2009) and Mennekens et al. (2010), however, have explored the SN Ia-rate using several progenitor scenarios (SD-Scenario, DD-Scenario and AM CVn). Both suggest that the SD-Scenario on its own can not explain the observed SNe Ia rate. The rate of the DD-Scenario seems to be much closer to the observed frequency. Possibly a mix of all channels is required to explain the observed rate.

In addition to the standard SD and DD channels, alternative scenarios are continually being explored. For example, a *core-degenerate* scenario in which a white dwarf merges with the hot core of a massive AGB star (Ilkov & Soker, 2011). Another alternative is given by Di Stefano et al. (2011) and Justham (2011), who suggest that the accreting white dwarf would be spun-up during accretion. The ignition of these highly spinning white dwarfs would be delayed and the companion might have time to evolve substantially from its RLOF phase.

van Kerkwijk et al. (2010) explores the merger of two equal mass white dwarfs with a total mass less than the Chandrasekhar mass. When coupled with the work on sub-Chandrasekhar mass detonations by Sim et al. (2010), this might actually provide a viable progenitor scenario. Its main advantage is the predicted rate of these low-mass white dwarf mergers might be high enough to reproduce the observations, but it is yet unclear if the conditions for an ignition can be reached in such a merger.

In summary, the question of the progenitors of SNe Ia remains one of the most highly debated topics in SNe Ia research. We have not yet found a scenario that elegantly explains all aspects of the SN Ia phenomenon. In addition, different measurements seem to provide conflicting evidence for either scenario. More extensive and novel observations of SNe Ia and SNR will hopefully identify the nature of SN Ia progenitors scenario.

1.6. Thesis motivation

One of the pivotal moments in astronomy in recent years was the discovery of the accelerating expansion of the universe by Riess et al. (1998) and Perlmutter et al. (1999). This discovery made SNe Ia the cynosure of the astronomical community. There have been many advances in recent years in the understanding of these cataclysmic events (explosion models, rates, etc.). One critical piece of the puzzle, however, has so far eluded discovery: the progenitors of SNe Ia. This work's main aim is to look for evidence for one SN Ia progenitor scenario. The SD-Scenario proposes a white dwarf accreting from a non-degenerate donor star. All calculations suggest that this donor star will survive

the explosion and would be visible thereafter. We have tried to find this companion in two of the three easily accessible ancient supernova remnants (SN 1572 and SN 1006). In Chapter **??** we have obtained spectra of Tycho-G, which had been suggested as the donor star of SN1572 (Ruiz-Lapuente et al., 2004). Although we confirmed some of the suggested parameters, we could not reproduce the unusually high radial velocity, which led to the claim. We also showed that the star exhibited no rotation, at odds with the star being the donor star.

We revisited SN 1572 in Chapter **??** with new observations of Tycho-G and five other stars in the neighbourhood of SN 1572. This work indicates Tycho-G is consistent with a background interloper, and is likely not to be the donor star (although it is hard to completely rule any star out). We discovered a curious A-star located right in the centre of SN1572. Despite its a priori unusual parameters, we are unable to reconcile this star (Tycho-B) with any feasible progenitor model.

SN 1006 provides an additional opportunity to search for progenitor stars. It is the closest known remnant of a SN Ia (2 kpc) and is largely unreddened. We have obtained 80 spectra of stars close to the centre of the remnant and present them in Chapter **??**. Again we do not find any obvious donor stars. We have obtained spectra of stars around SN 1604 but these are not presented in this thesis. They will be analysed as part of future work.

Progenitor hunts provide us with information of the scenarios pre-explosion. Spectra, on the other hand, help to unravel the physics during and post-explosion. Mazzali et al. (2008) have developed a code that can produce synthetic SN Ia spectra from fundamental input parameters. Fitting an observed SN Ia is, for the moment, a manual task. This requires many days, if not weeks, of tweaking. The deluge of spectroscopically well-sampled SNe Ia from surveys is already upon us. Manual analysis of all of these spectra is impossible. The information about the explosion hidden in the spectra is, however, crucial to our understanding of these events. In Chapter **??** we present our work towards automating this fitting process. We have tried a variety of algorithms to explore the vast and extremely complex search space. Working together with members of the computer science community, we are exploring the use of genetic algorithms to solve this problem. This thesis does not attempt to completely solve this problem, but we present preliminary methods in SN Ia-fitting in Chapter **??**. When completed, we can apply this method not only to fitting SN Ia, but fitting different supernovae and to other areas of astronomy.

In summary, this work explores two areas of supernova physics: progenitors and explosion physics. The hunt for progenitors has not yielded obvious candidates, but may suggest a rethinking of the 'normal' SD-Scenario. The automated fitting of supernova spectra is in a preliminary stage. We have, however, shown that it is possible to explore the parameter space in an automated fashion. This will hopefully yield elemental abundances and energies for many thousands of supernovae. The close collaboration with computer science community was very helpful and shows how important cross-disciplinary research is in the modern era of science.

Bibliography

Abramovici, A., et al. 1992, Science, 256, 325 (ADS entry)

Aldering, G., et al. 2002, in Presented at the Society of Photo-Optical Instrumentation Engineers (SPIE) Conference, Vol. 4836, Society of Photo-Optical Instrumentation Engineers (SPIE) Conference Series, ed. J. A. Tyson & S. Wolff, 61–72 (ADS entry)

Alekseev, E. N., Alekseeva, L. N., Krivosheina, I. V., & Volchenko, V. I. 1988, Phys. Lett., B205, 209

Arnett, W. D. 1969, Ap&SS, 5, 180 (ADS entry)

—. 1982, ApJ, 253, 785 (ADS entry)

Astier, P., Guy, J., Pain, R., & Balland, C. 2011, A&A, 525, A7+ (ADS entry)

Baade, W. 1938, ApJ, 88, 285 (ADS entry)

Baade, W., & Zwicky, F. 1934, Proceedings of the National Academy of Science, 20, 254 (ADS entry)

Badenes, C., Borkowski, K. J., & Bravo, E. 2005, ApJ, 624, 198 (ADS entry)

Badenes, C., Borkowski, K. J., Hughes, J. P., Hwang, U., & Bravo, E. 2006, ApJ, 645, 1373 (ADS entry)

Badenes, C., Bravo, E., Borkowski, K. J., & Domínguez, I. 2003, ApJ, 593, 358 (ADS entry)

Barbary, K., et al. 2010, ArXiv e-prints (ADS entry)

Barbon, R., Ciatti, F., & Rosino, L. 1979, A&A, 72, 287 (ADS entry)

Belokurov, V. A., & Evans, N. W. 2003, MNRAS, 341, 569 (ADS entry)

Benetti, S., et al. 2004, MNRAS, 348, 261 (ADS entry)

—. 2005, ApJ, 623, 1011 (ADS entry)

Bianco, F. B., et al. 2011, ArXiv e-prints (ADS entry)

Bildsten, L., Shen, K. J., Weinberg, N. N., & Nelemans, G. 2007, ApJ, 662, L95 (ADS entry)

Bionta, R. M., Blewitt, G., Bratton, C. B., Casper, D., & Ciocio, A. 1987, Physical Review Letters, 58, 1494 (ADS entry)

Blake, C., et al. 2011, MNRAS, 951 (ADS entry)

Blondin, J. M., & Mezzacappa, A. 2006, ApJ, 642, 401 (ADS entry)

Brahe, T., & Kepler, J. 1602, Tychonis Brahe Astronomiae instauratae progymnasmata : quorum haec prima pars de restitutione motuum SOLIS et lunae stellarumque inerrantium tractat, et praeterea de admiranda nova stella anno 1572 exorta luculenter agit., ed. Brahe, T. & Kepler, J. (ADS entry)

Branch, D., Fisher, A., & Nugent, P. 1993, AJ, 106, 2383 (ADS entry)

Branch, D., & Tammann, G. A. 1992, ARA&A, 30, 359 (ADS entry)

Burrows, A., Livne, E., Dessart, L., Ott, C. D., & Murphy, J. 2007, ApJ, 655, 416 (ADS entry)

Canal, R., Méndez, J., & Ruiz-Lapuente, P. 2001, ApJ, 550, L53 (ADS entry)

Chandrasekhar, S. 1931, ApJ, 74, 81 (ADS entry)

Chin, Y.-N., & Huang, Y.-L. 1994, Nature, 371, 398 (ADS entry)

Clark, D. H., & Stephenson, F. R. 1977, The historical supernovae, ed. Clark, D. H. & Stephenson, F. R. (ADS entry)

Colgate, S. A. 1974, ApJ, 187, 333 (ADS entry)

Colgate, S. A., Moore, E. P., & Carlson, R. 1975, PASP, 87, 565 (ADS entry)

Di Stefano, R. 2010, ApJ, 719, 474 (ADS entry)

Di Stefano, R., Kong, A., & Primini, F. A. 2006, ArXiv Astrophysics e-prints (ADS entry)

Di Stefano, R., Voss, R., & Claeys, J. S. W. 2011, ArXiv e-prints (ADS entry)

Dotani, T., Hayashida, K., Inoue, H., Itoh, M., & Koyama, K. 1987, Nature, 330, 230 (ADS entry)

Einstein, A. 1918, Sitzungsberichte der Königlich Preußischen Akademie der Wissenschaften (Berlin), Seite 154-167., 154 (ADS entry)

Ensman, L., & Burrows, A. 1992, ApJ, 393, 742 (ADS entry)

Filippenko, A. V., Li, W. D., Treffers, R. R., & Modjaz, M. 2001, in Astronomical Society of the Pacific Conference Series, Vol. 246, IAU Colloq. 183: Small Telescope Astronomy on Global Scales, ed. B. Paczynski, W.-P. Chen, & C. Lemme, 121–+ (ADS entry)

Filippenko, A. V., et al. 1992, AJ, 104, 1543 (ADS entry)

Fink, M., Röpke, F. K., Hillebrandt, W., Seitenzahl, I. R., Sim, S. A., & Kromer, M. 2010, A&A, 514, A53+ (ADS entry)

Galama, T. J., et al. 1998, Nature, 395, 670 (ADS entry)

Ganeshalingam, M., Li, W., & Filippenko, A. V. 2011, ArXiv e-prints (ADS entry)

Garavini, G., et al. 2007, A&A, 471, 527 (ADS entry)

Garnavich, P. M., et al. 2002, in Bulletin of the American Astronomical Society, Vol. 34, American Astronomical Society Meeting Abstracts, 1233–+ (ADS entry)

Gaskell, C. M., Cappellaro, E., Dinerstein, H. L., Garnett, D. R., Harkness, R. P., & Wheeler, J. C. 1986, ApJ, 306, L77 (ADS entry)

Genet, R. M., Boyd, L. J., & Hall, D. S. 1986, in IAU Symposium, Vol. 118, Instrumentation and Research Programmes for Small Telescopes, ed. J. B. Hearnshaw & P. L. Cottrell, 47–54 (ADS entry)

Gerardy, C. L., et al. 2004, ApJ, 607, 391 (ADS entry)

Gilfanov, M., & Bogdán, Á. 2010, Nature, 463, 924 (ADS entry)

Goldstein, B. R. 1965, AJ, 70, 105 (ADS entry)

Green, D. A., & Gull, S. F. 1984, Nature, 312, 527 (ADS entry)

Green, D. A., & Stephenson, F. R. 2003, in Lecture Notes in Physics, Berlin Springer Verlag, Vol. 598, Supernovae and Gamma-Ray Bursters, ed. K. Weiler, 7–19 (ADS entry)

Gutiérrez, J., Canal, R., & García-Berro, E. 2005, A&A, 435, 231 (ADS entry)

Guy, J., et al. 2007, A&A, 466, 11 (ADS entry)

Hachinger, S., Mazzali, P. A., Taubenberger, S., Pakmor, R., & Hillebrandt, W. 2009, MNRAS, 399, 1238 (ADS entry)

Hachisu, I., Kato, M., & Nomoto, K. 2008, ApJ, 683, L127 (ADS entry)

Hamuy, M., Phillips, M. M., Maza, J., Suntzeff, N. B., Schommer, R. A., & Aviles, R. 1995, AJ, 109, 1 (ADS entry)

Hamuy, M., & Pinto, P. A. 2002, ApJ, 566, L63 (ADS entry)

Hamuy, M., et al. 1993, AJ, 106, 2392 (ADS entry)

Han, Z. 2008, ApJ, 677, L109 (ADS entry)

Han, Z., & Podsiadlowski, P. 2004, MNRAS, 350, 1301 (Link)

Hanbury Brown, R., & Hazard, C. 1952, Nature, 170, 364 (ADS entry)

Hancock, P., Gaensler, B. M., & Murphy, T. 2011, ArXiv e-prints (ADS entry)

Harkness, R. P., et al. 1987, ApJ, 317, 355 (ADS entry)

Hartwig, E. 1885, Astronomische Nachrichten, 112, 360 (ADS entry)

Hatano, K., Branch, D., Fisher, A., Baron, E., & Filippenko, A. V. 1999, ApJ, 525, 881 (ADS entry)

Hayden, B. T., et al. 2010, ApJ, 722, 1691 (ADS entry)

Herant, M., Benz, W., Hix, W. R., Fryer, C. L., & Colgate, S. A. 1994, ApJ, 435, 339 (ADS entry)

Hicken, M., Garnavich, P. M., Prieto, J. L., Blondin, S., DePoy, D. L., Kirshner, R. P., & Parrent, J. 2007, ApJ, 669, L17 (ADS entry)

Hillebrandt, W., & Niemeyer, J. C. 2000, ARA&A, 38, 191 (ADS entry)

Hirashita, H., Buat, V., & Inoue, A. K. 2003, A&A, 410, 83 (ADS entry)

Hirata, K., Kajita, T., Koshiba, M., Nakahata, M., & Oyama, Y. 1987, Physical Review Letters, 58, 1490 (ADS entry)

Howell, D. A., et al. 2006, Nature, 443, 308 (ADS entry)

Hubble, E. 1929, Proceedings of the National Academy of Science, 15, 168 (ADS entry)

Hubble, E. P. 1926, ApJ, 64, 321 (ADS entry)

Iben, Jr., I., & Tutukov, A. V. 1984, ApJS, 54, 335 (ADS entry)

Iliadis, C. 2007, Nuclear Physics of Stars, ed. Iliadis, C. (Wiley-VCH Verlag) (ADS entry)

Ilkov, M., & Soker, N. 2011, ArXiv e-prints (ADS entry)

Jafry, Y. R., Cornelisse, J., & Reinhard, R. 1994, ESA Journal, 18, 219 (ADS entry)

Jha, S., Riess, A. G., & Kirshner, R. P. 2007, ApJ, 659, 122 (ADS entry)

Justham, S. 2011, ApJ, 730, L34+ (ADS entry)

Justham, S., Wolf, C., Podsiadlowski, P., & Han, Z. 2009, A&A, 493, 1081 (ADS entry)

Kaiser, N. 2004, in Presented at the Society of Photo-Optical Instrumentation Engineers (SPIE) Conference, Vol. 5489, Society of Photo-Optical Instrumentation Engineers (SPIE) Conference Series, ed. J. M. Oschmann Jr., 11–22 (ADS entry)

Karle, A. 2008, in International Cosmic Ray Conference, Vol. 4, International Cosmic Ray Conference, 835–838 (ADS entry)

Kasen, D. 2006, ApJ, 649, 939 (ADS entry)

—. 2010, ApJ, 708, 1025 (ADS entry)

Kasen, D., Röpke, F. K., & Woosley, S. E. 2009, Nature, 460, 869 (ADS entry)

Keller, S. C., et al. 2007, PASA, 24, 1 (ADS entry)

Kepler, J. 1606, De Stella nova in pede Serpentarii

Kepler, S. O., Kleinman, S. J., Nitta, A., Koester, D., Castanheira, B. G., Giovannini, O., Costa, A. F. M., & Althaus, L. 2007, MNRAS, 375, 1315 (ADS entry)

Kerzendorf, W. E., Schmidt, B. P., Asplund, M., Nomoto, K., Podsiadlowski, P., Frebel, A., Fesen, R. A., & Yong, D. 2009, ApJ, 701, 1665 (ADS entry)

Kirshner, R. P., & Kwan, J. 1974, ApJ, 193, 27 (ADS entry)

Klebesadel, R. W., Strong, I. B., & Olson, R. A. 1973, ApJ, 182, L85+ (ADS entry)

Klein, R. I., & Chevalier, R. A. 1978, ApJ, 223, L109 (ADS entry)

Komatsu, E., et al. 2011, ApJS, 192, 18 (ADS entry)

Kowal, C. T. 1968, AJ, 73, 1021 (ADS entry)

Kozma, C., Fransson, C., Hillebrandt, W., Travaglio, C., Sollerman, J., Reinecke, M., Röpke, F. K., & Spyromilio, J. 2005, A&A, 437, 983 (ADS entry)

Krause, O., Tanaka, M., Usuda, T., Hattori, T., Goto, M., Birkmann, S., & Nomoto, K. 2008, Nature, 456, 617 (ADS entry)

Leibundgut, B., & Tammann, G. A. 1990, A&A, 230, 81 (ADS entry)

Leloudas, G., et al. 2009, A&A, 505, 265 (ADS entry)

Leonard, D. C. 2007, ApJ, 670, 1275 (ADS entry)

Lesaffre, P., Podsiadlowski, P., & Tout, C. A. 2005, Nuclear Physics A, 758, 463 (ADS entry)

Li, W., et al. 2003, PASP, 115, 453 (ADS entry)

—. 2011, MNRAS, 412, 1441 (ADS entry)

Li, W. D., et al. 2000, in American Institute of Physics Conference Series, Vol. 522, American Institute of Physics Conference Series, ed. S. S. Holt & W. W. Zhang, 103–106 (ADS entry)

Livne, E. 1990, ApJ, 354, L53 (ADS entry)

Livne, E., & Arnett, D. 1995, ApJ, 452, 62 (ADS entry)

Mandel, K. S., Narayan, G., & Kirshner, R. P. 2011, ApJ, 731, 120 (ADS entry)

Mannucci, F., Della Valle, M., & Panagia, N. 2006, MNRAS, 370, 773 (ADS entry)

Mannucci, F., Della Valle, M., Panagia, N., Cappellaro, E., Cresci, G., Maiolino, R., Petrosian, A., & Turatto, M. 2005, A&A, 433, 807 (ADS entry)

Maoz, D., & Badenes, C. 2010, MNRAS, 407, 1314 (ADS entry)

Maoz, D., Sharon, K., & Gal-Yam, A. 2010, ApJ, 722, 1879 (ADS entry)

Marietta, E., Burrows, A., & Fryxell, B. 2000, ApJS, 128, 615 (ADS entry)

Mazzali, P. A., Röpke, F. K., Benetti, S., & Hillebrandt, W. 2007, Science, 315, 825 (ADS entry)

Mazzali, P. A., Sauer, D. N., Pastorello, A., Benetti, S., & Hillebrandt, W. 2008, MNRAS, 386, 1897 (ADS entry)

Mazzali, P. A., et al. 2005, ApJ, 623, L37 (ADS entry)

Meegan, C. A., Fishman, G. J., Wilson, R. B., Horack, J. M., Brock, M. N., Paciesas, W. S., Pendleton, G. N., & Kouveliotou, C. 1992, Nature, 355, 143 (ADS entry)

Meikle, W. P. S. 2000, MNRAS, 314, 782 (ADS entry)

Mennekens, N., Vanbeveren, D., De Greve, J. P., & De Donder, E. 2010, A&A, 515, A89+ (ADS entry)

Miller, D. L., & Branch, D. 1990, AJ, 100, 530 (ADS entry)

Minkowski, R. 1941, PASP, 53, 224 (ADS entry)

Nelemans, G. 2005, in Astronomical Society of the Pacific Conference Series, Vol. 330, The Astrophysics of Cataclysmic Variables and Related Objects, ed. J.-M. Hameury & J.-P. Lasota, 27–+ (ADS entry)

Nomoto, K. 1982, ApJ, 253, 798 (Link)

Nomoto, K., & Kondo, Y. 1991, ApJ, 367, L19 (ADS entry)

Norgaard-Nielsen, H. U., Hansen, L., Jorgensen, H. E., Aragon Salamanca, A., & Ellis, R. S. 1989, Nature, 339, 523 (ADS entry)

Nugent, P., Phillips, M., Baron, E., Branch, D., & Hauschildt, P. 1995, ApJ, 455, L147+ (ADS entry)

Nugent, P., et al. 2006, ApJ, 645, 841 (ADS entry)

Pain, R., & SNLS Collaboration. 2003, in Bulletin of the American Astronomical Society, Vol. 35, American Astronomical Society Meeting Abstracts, 1335–+ (ADS entry)

Pakmor, R., Kromer, M., Röpke, F. K., Sim, S. A., Ruiter, A. J., & Hillebrandt, W. 2010, Nature, 463, 61 (ADS entry)

Pakmor, R., Röpke, F. K., Weiss, A., & Hillebrandt, W. 2008, A&A, 489, 943 (ADS entry)

Patat, F., Chugai, N. N., Podsiadlowski, P., Mason, E., Melo, C., & Pasquini, L. 2011, A&A, 530, A63+ (ADS entry)

Patat, F., et al. 2007, Science, 317, 924 (ADS entry)

Perlmutter, S., et al. 1995, NASA STI/Recon Technical Report N, 96, 29501 (ADS entry)

—. 1999, ApJ, 517, 565 (ADS entry)

Perryman, M. A. C., et al. 2001, A&A, 369, 339 (ADS entry)

Phillips, M. M. 1993, ApJ, 413, L105 (ADS entry)

Phillips, M. M., Wells, L. A., Suntzeff, N. B., Hamuy, M., Leibundgut, B., Kirshner, R. P., & Foltz, C. B. 1992, AJ, 103, 1632 (ADS entry)

Pinto, P. A., & Eastman, R. G. 2000, ApJ, 530, 757 (ADS entry)

Pinto, P. A., et al. 2006, in Bulletin of the American Astronomical Society, Vol. 38, American Astronomical Society Meeting Abstracts, 1017–+ (ADS entry)

Podsiadlowski, P., Joss, P. C., & Hsu, J. J. L. 1992, ApJ, 391, 246 (ADS entry)

Quimby, R., Höflich, P., Kannappan, S. J., Rykoff, E., Rujopakarn, W., Akerlof, C. W., Gerardy, C. L., & Wheeler, J. C. 2006, ApJ, 636, 400 (ADS entry)

Rau, A., et al. 2009, PASP, 121, 1334 (ADS entry)

Rest, A., et al. 2005, Nature, 438, 1132 (ADS entry)

—. 2008a, ApJ, 681, L81 (ADS entry)

—. 2008b, ApJ, 680, 1137 (ADS entry)

—. 2011, ApJ, 732, 3 (ADS entry)

Reynolds, S. P., Borkowski, K. J., Green, D. A., Hwang, U., Harrus, I., & Petre, R. 2008, ApJ, 680, L41 (ADS entry)

Reynolds, S. P., Borkowski, K. J., Hwang, U., Hughes, J. P., Badenes, C., Laming, J. M., & Blondin, J. M. 2007, ApJ, 668, L135 (ADS entry)

Richmond, M., Treffers, R. R., & Filippenko, A. V. 1993, PASP, 105, 1164 (ADS entry)

Riess, A. G., Press, W. H., & Kirshner, R. P. 1996, ApJ, 473, 88 (ADS entry)

Riess, A. G., et al. 1998, AJ, 116, 1009 (ADS entry)

—. 1999, AJ, 118, 2675 (ADS entry)

Ritossa, C., Garcia-Berro, E., & Iben, Jr., I. 1996, ApJ, 460, 489 (ADS entry)

Roelofs, G., Bassa, C., Voss, R., & Nelemans, G. 2008, MNRAS, 391, 290 (ADS entry)

Röpke, F. K., & Bruckschen, R. 2008, New Journal of Physics, 10, 125009 (ADS entry)

Röpke, F. K., & Hillebrandt, W. 2005, A&A, 431, 635 (ADS entry)

Ruiter, A. J., Belczynski, K., & Fryer, C. 2009, ApJ, 699, 2026 (ADS entry)

Ruiz-Lapuente, P., et al. 2004, Nature, 431, 1069 (ADS entry)

Scalzo, R. A., et al. 2010, ApJ, 713, 1073 (ADS entry)

Schlegel, E. M. 1990, MNRAS, 244, 269 (ADS entry)

Schmidt, B. P., Kirshner, R. P., Eastman, R. G., Phillips, M. M., Suntzeff, N. B., Hamuy, M., Maza, J., & Aviles, R. 1994a, ApJ, 432, 42 (ADS entry)

Schmidt, B. P., Kirshner, R. P., Leibundgut, B., Wells, L. A., Porter, A. C., Ruiz-Lapuente, P., Challis, P., & Filippenko, A. V. 1994b, ApJ, 434, L19 (ADS entry)

Schmidt, W., Ciaraldi-Schoolmann, F., Niemeyer, J. C., Röpke, F. K., & Hillebrandt, W. 2010, ApJ, 710, 1683 (ADS entry)

Schweizer, F., & Middleditch, J. 1980, ApJ, 241, 1039 (ADS entry)

Shigeyama, T., Nomoto, K., Yamaoka, H., & Thielemann, F.-K. 1992, ApJ, 386, L13 (ADS entry)

Silverman, J. M., Ganeshalingam, M., Li, W., Filippenko, A. V., Miller, A. A., & Poznanski, D. 2011, MNRAS, 410, 585 (ADS entry)

Sim, S. A., Röpke, F. K., Hillebrandt, W., Kromer, M., Pakmor, R., Fink, M., Ruiter, A. J., & Seitenzahl, I. R. 2010, ApJ, 714, L52 (ADS entry)

Smartt, S. J. 2009, ARA&A, 47, 63 (ADS entry)

Soderberg, A. M., Nakar, E., Berger, E., & Kulkarni, S. R. 2006, ApJ, 638, 930 (ADS entry)

Soderberg, A. M., et al. 2008, Nature, 453, 469 (ADS entry)

—. 2010, Nature, 463, 513 (ADS entry)

Sorokina, E. I., Blinnikov, S. I., Kosenko, D. I., & Lundqvist, P. 2004, Astronomy Letters, 30, 737 (ADS entry)

Staelin, D. H., & Reifenstein, III, E. C. 1968, Science, 162, 1481 (ADS entry)

Stehle, M., Mazzali, P. A., Benetti, S., & Hillebrandt, W. 2005, MNRAS, 360, 1231 (ADS entry)

Sternberg, A., et al. 2011, ArXiv e-prints (ADS entry)

Strolger, L.-G., et al. 2004, ApJ, 613, 200 (ADS entry)

Sullivan, M., et al. 2011, ArXiv e-prints (ADS entry)

Sunyaev, R., et al. 1987, Nature, 330, 230 (ADS entry)

Tammann, G. A., Loeffler, W., & Schroeder, A. 1994, ApJS, 92, 487 (ADS entry)

Tanaka, M., Mazzali, P. A., Maeda, K., & Nomoto, K. 2006, ApJ, 645, 470 (ADS entry)

Tanaka, M., Mazzali, P. A., Stanishev, V., Maurer, I., Kerzendorf, W. E., & Nomoto, K. 2011, MNRAS, 410, 1725 (ADS entry)

Tanaka, M., et al. 2010, ApJ, 714, 1209 (ADS entry)

Taubenberger, S., et al. 2011, MNRAS, 412, 2735 (ADS entry)

Thomas, R. C., Branch, D., Baron, E., Nomoto, K., Li, W., & Filippenko, A. V. 2004, ApJ, 601, 1019 (ADS entry)

Totani, T., Morokuma, T., Oda, T., Doi, M., & Yasuda, N. 2008, PASJ, 60, 1327 (ADS entry)

Turatto, M. 2003, in Lecture Notes in Physics, Berlin Springer Verlag, Vol. 598, Supernovae and Gamma-Ray Bursters, ed. K. Weiler, 21–36 (ADS entry)

Turatto, M., Benetti, S., & Pastorello, A. 2007, in American Institute of Physics Conference Series, Vol. 937, Supernova 1987A: 20 Years After: Supernovae and Gamma-Ray Bursters, ed. S. Immler, K. Weiler, & R. McCray, 187–197 (ADS entry)

Umeda, H., & Yoshida, T. 2010, in American Institute of Physics Conference Series, Vol. 1279, American Institute of Physics Conference Series, ed. N. Kawai & S. Nagataki, 171–178 (ADS entry)

van den Bergh, S. 1960, ZAp, 49, 201 (ADS entry)

van den Bergh, S., & Tammann, G. A. 1991, ARA&A, 29, 363 (ADS entry)

van den Heuvel, E. P. J., Bhattacharya, D., Nomoto, K., & Rappaport, S. A. 1992, A&A, 262, 97 (ADS entry)

van Dyk, S. D., Treffers, R. R., Richmond, M. W., Filippenko, A. V., & Paik, Y. 1994, in Bulletin of the American Astronomical Society, Vol. 26, American Astronomical Society Meeting Abstracts, 1444–+ (ADS entry)

van Kerkwijk, M. H., Chang, P., & Justham, S. 2010, ApJ, 722, L157 (ADS entry)

Voss, R., & Nelemans, G. 2008, Nature, 451, 802 (ADS entry)

Walborn, N. R., Prevot, M. L., Prevot, L., Wamsteker, W., Gonzalez, R., Gilmozzi, R., & Fitzpatrick, E. L. 1989, A&A, 219, 229 (ADS entry)

Webbink, R. F. 1984, ApJ, 277, 355 (ADS entry)

Whelan, J., & Iben, Jr., I. 1973, ApJ, 186, 1007 (ADS entry)

Wood-Vasey, W. M., et al. 2008, ApJ, 689, 377 (ADS entry)

Woosley, S. E., Heger, A., & Weaver, T. A. 2002, Reviews of Modern Physics, 74, 1015 (ADS entry)

Wu, C.-C., Crenshaw, D. M., Hamilton, A. J. S., Fesen, R. A., Leventhal, M., & Sarazin, C. L. 1997, ApJ, 477, L53+ (ADS entry)

Wu, C.-C., Leventhal, M., Sarazin, C. L., & Gull, T. R. 1983, ApJ, 269, L5 (ADS entry)

Xu, D., et al. 2009, ApJ, 696, 971 (ADS entry)

Yamanaka, M., et al. 2009, ApJ, 707, L118 (ADS entry)

Yoon, S.-C., & Langer, N. 2004, A&A, 419, 623 (ADS entry)

—. 2005, A&A, 435, 967 (ADS entry)

Zhang, B., Dai, X., Lloyd-Ronning, N. M., & Mészáros, P. 2004, ApJ, 601, L119 (ADS entry)

Zhao, F., Strom, R. G., & Jiang, S. 2006, Chinese J. Astron. Astrophys., 6, 635 (ADS entry)

Zwicky, F. 1938, ApJ, 88, 529 (ADS entry)

—. 1940, Reviews of Modern Physics, 12, 66 (ADS entry)